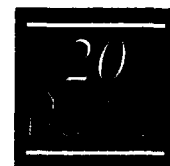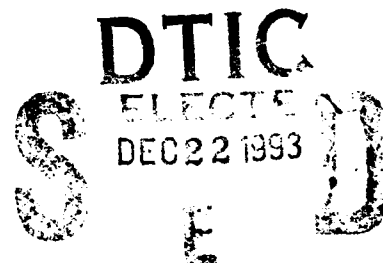NASA Contractor Report 191536

ICASE Report No. 93-69

AD-A273 992

ICASE

SIMULATIONS OF DIFFUSION-REACTION EQUATIONS WITH IMPLICATIONS TO TURBULENT COMBUSTION MODELING

Sharath S. Girimaji

DTIC
ELECTE
DEC 22 1993
E

93-30651

National Aeronautics and
Space Administration

Langley Research Center
Hampton, Virginia 23681-0001

93 12 17 049

ICASE Fluid Mechanics

Due to increasing research being conducted at ICASE in the field of fluid mechanics, future ICASE reports in this area of research will be printed with a green cover. Applied and numerical mathematics reports will have the familiar blue cover, while computer science reports will have yellow covers. In all other aspects the reports will remain the same; in particular, they will continue to be submitted to the appropriate journals or conferences for formal publication.

Accesion For		
NTIS CRA&I		☒
DTIC TAB		☐
Unannounced		☐
Justification		
By		
Distribution /		
Availability Codes		
Dist	Avail and / or Special	
A-1		

DTIC QUALITY INSPECTED 3

SIMULATIONS OF DIFFUSION-REACTION EQUATIONS WITH IMPLICATIONS TO TURBULENT COMBUSTION MODELING

Sharath S. Girimaji[1]

Institute for Computer Applications in Science and Engineering

NASA Langley Research Center

Hampton, VA 23681

ABSTRACT

An enhanced diffusion-reaction reaction system (DRS) is proposed as a statistical model for the evolution of multiple scalars undergoing mixing and reaction in an isotropic turbulence field. The DRS model is close enough to the scalar equations in a reacting flow that other statistical models of turbulent mixing that decouple the velocity field from scalar mixing and reaction (e.g. mapping closure model, assumed-pdf models) cannot distinguish the model equations from the original equations. Numerical simulations of DRS are performed for three scalars evolving from non-premixed initial conditions. A simple one-step reversible reaction is considered. The data from the simulations are used (i) to study the effect of chemical conversion on the evolution of scalar statistics, and (ii) to evaluate other models (mapping-closure model, assumed multivariate β-pdf model).

1 Introduction

Turbulent combustion is an interplay of several complex physical processes: e.g. turbulent transport, scalar mixing, chemical reaction, heat release. Turbulent transport is present only in inhomogeneous flows where the gradients of the scalar statistics are non-zero. Scalar mixing– which is important in isotropic as well as inhomogeneous flows– comprises two mechanisms: the effect of the velocity field, which is to cascade scalar energy to smaller length scales; and molecular diffusion, which typically acts at smaller scales to reduce scalar fluctuations. Chemical reaction is a local phenomenon which converts scalar species from reactants to products. In problems of interest in combustion, chemical conversion is accompanied by heat release and, hence, density reduction. If the heat release is large enough, the resulting buoyancy forces can modify the velocity field in which the scalars reside. If the heat release is small, the modification of the velocity field is negligible.

In the scalar-statistics equations, the terms representing several of the above processes need closure modeling. A turbulent combustion model is really a composite of these closure models of the individual processes. Often, when calculations from the composite model are in poor agreement with either experimental or direct numerical simulation (DNS) data, it is difficult to isolate the underlying cause (the model of a specific physical process) of the disagreement. For this reason, it is useful to construct sample test problems where only one or few of the physical processes are important (other processes are either negligible or or completely absent). Data from the numerical simulations of such a test problem can be used to construct and validate the individual models.

The divide-and-conquer approach has proved especially successful in the understanding and modeling of the inert scalar mixing process. Eswaran and Pope (1988), and subsequently others, performed DNS of inert scalar fields evolving from non-premixed initial conditions in constant-density, isotropic turbulence. In this first step, the effect of velocity field on scalar mixing is studied, without the complexities of spatial inhomogeneities or chemical reaction. One of the chief findings of DNS studies is that (for the range of Reynolds number investigated, R_λ 30 - 90) the velocity field only affects the timescale of the scalar pdf evolution. In appropriately normalized time, the scalar pdf evolution is independent of the velocity

field. This insight gained from the DNS studies spawned reasonably successful modeling approaches in which the scalar evolution is considered only in the normalized time, thus decoupling the velocity field from the scalar field. The models are: the mapping closure model (Kraichnan 1989, Girimaji 1992b), the Johnson-Edgeworth translation (JET) models of Madnia *et al* (1992) and the assumed β-pdf model (Girimaji 1991a).

Study of a test case which combines scalar mixing with chemical chemical reaction in isotropic turbulence should be a useful second step towards the ultimate objective of understanding and modeling turbulent combustion. In this work, we analyze the test-case equations and propose a statistical model for the scalar (species and temperature) evolution. The model equation set is a diffusion-reaction system (DRS). The model accounts for the effect of the velocity field via a time-dependent diffusion enhancement coefficient factor. The model equations are close enough to the original turbulent-reaction equations that other models which decouple the velocity field and scalar-field mixing cannot distinguish between the two sets of equations. Numerical simulation of the model DRS equations is computationally much less intensive than DNS of the original equations and may serve nearly as useful a purpose in understanding and evaluating turbulent combustion models. Simulations of the DRS equations are performed to (i) shed some light on the effect of reaction on scalar field evolution, and (ii) evaluate the performance of other models (developed originally for inert mixing) against reacting scalar data.

The organization of the remainder of the paper is as follows. In Section 2, the relevance of the (enhanced) DRS to turbulent combustion is investigated in more detail. Numerical simulations of DRS equations is performed in in section 3. A brief description of the numerics employed in the simulations is also provided. Section 4 contains the results of the simulation and a discussion of its implications to turbulent combustion modeling. The paper concludes in Section 5 with a summary.

2 Enhanced diffusion-reaction system as a model of turbulent reactive flows

Consider the mixing and reaction of n scalars (of mass fractions ϕ_α, $\alpha = 1, \cdots n$) in a velocity field $\mathbf{u}(\mathbf{X}, t)$ evolving under Navier-Stokes. The following assumptions are made: i) no body force, ii) no radiative heat transfer, iii) scalar diffusion governed by Fickian law, iv) low Mach number (hence, pressure is considered nearly a constant), and v) high Reynolds number (hence, the viscous contribution to the energy equation is negligible). Subject to the above assumptions, the scalar and temperature (T) evolution equations are

$$\rho[\frac{\partial \phi_\alpha}{\partial t} + u_i \frac{\partial \phi_\alpha}{\partial X_i}] = \frac{\partial}{\partial X_i}[\rho D_\alpha \frac{\partial \phi_\alpha}{\partial X_i}] + w_\alpha, \tag{1}$$

and

$$\rho[\frac{\partial h^T}{\partial t} + u_i \frac{\partial h^T}{\partial X_i}] = \frac{\partial}{\partial X_i}[\lambda \frac{\partial T}{\partial X_i}] + \sum_{\alpha=1}^{n} \frac{\partial}{\partial X_i}[\rho h_\alpha^T D_\alpha \frac{\partial \phi_\alpha}{\partial X_i}] - \sum_{\alpha=1}^{n} h_\alpha^0 w_\alpha. \tag{2}$$

In the above equations, D_α and w_α are respectively the Fickian diffusion coefficient and the chemical production rate of species α. The heat conductivity of the mixture is λ. The enthaly of formation and thermal enthaly of species α are h_α^0 and h_α^T. The total thermal enthalpy of the mixture, (h^T), is given by

$$h^T = \sum_{\alpha=1}^{n} \phi_\alpha h_\alpha^T. \tag{3}$$

The pressure (p), density of the mixture (ρ) and the mass fractions are related through the equation of state which could be the ideal gas law. It is assumed that the temperature and the chemical source terms can be determined given the thermal enthalpy and mass fractions.

Subject to homogeniety of the turbulent velocity field, the joint pdf of scalar composition and thermal enthalpy, $F(h^T, \underline{\phi})$, evolves according to (Pope 1985)

$$\rho(h^T, \underline{\phi}) \frac{\partial F(h^T, \underline{\phi})}{\partial t} = - \frac{\partial}{\partial h^T}[F(T, \underline{\phi})\{\Theta_T - R_T\}] \tag{4}$$

$$- \sum_{\alpha=1}^{n} \frac{\partial}{\partial \phi_\alpha}[F(h^T, \underline{\phi})\{\Theta_{\phi\alpha} - R_{\phi\alpha}\}].$$

In the above equation the conditional diffusion of temperature (Θ_T) and scalar ($\Theta_{\phi\alpha}$) are given by

$$\Theta_T = \langle \frac{\partial}{\partial X_i}[\lambda \frac{\partial T}{\partial X_i} + \sum_{\alpha=1}^{n} \rho h_\alpha^T D_\alpha \frac{\partial \phi_\alpha}{\partial X_i}]|T, \underline{\phi} \rangle, \tag{5}$$

3

and

$$\Theta_{\phi\alpha} = \langle \frac{\partial}{\partial X_i}[D_\alpha \frac{\partial \phi_\alpha}{\partial X_i}]|T,\underline{\phi}\rangle, \tag{6}$$

where, the notation $\langle b|r \rangle$ denotes the conditional mean of b with respect to r. The pdf source term of temperature (R_T) and scalar ($R_{\phi\alpha}$) due to reaction are given by

$$R_T = -\sum_{\alpha=1}^{n} h_\alpha^0 w_\alpha, \tag{7}$$

and

$$R_{\phi\alpha} = w_\alpha. \tag{8}$$

While the source terms due to reaction are closed in terms of temperature and scalar composition, the scalar diffusion terms need closure modeling. The modeling of these terms require that the effect of the velocity field on the scalar field be known, at least approximately.

2.1 Lagrangian coordinate analysis

The effect of the velocity field on the scalar field is examined in Lagrangian frame of reference (x, t) which is cartesian. For the sake of this analysis, the velocity field is assumed to be isotropic. The Eulerian coordinate **X** is now nonstationary, curvilinear and nonorthogonal, evolving according to

$$\frac{\partial \mathbf{X}(\mathbf{x},t)}{\partial t} = \mathbf{U}[\mathbf{X}(\mathbf{x},t),t]. \tag{9}$$

The Eulerian conditional diffusion can now be written in terms of the Lagrangian derivatives:

$$\Theta_{\phi\alpha} = \langle \frac{\partial}{\partial X_i}[D_\alpha \frac{\partial \phi_\alpha}{\partial X_i}]|T,\underline{\phi}\rangle, = \langle \frac{\partial x_a}{\partial X_i}\frac{\partial x_b}{\partial X_i}\frac{\partial}{\partial x_a}[D_\alpha \frac{\partial \phi_\alpha}{\partial x_b}]|T,\underline{\phi}\rangle. \tag{10}$$

Define

$$C_{ai}(\mathbf{x}) = \frac{\partial x_a}{\partial X_i}. \tag{11}$$

The correlation between C_{ia} and the scalar derivatives in the Lagrangian coordinates is discussed in detail in Girimaji (1992 c) for the case of inert scalar mixing. It is pointed out that C_{ia} related to the rate at which the turbulence stretches a material surface attached to x. The determinant of C_{ia}, $|C|$, is likely to be larger than unity if the material surface is stretched by turbulence and smaller than unity if the surface is shrunk. On an average

4

turbulence stretches material surfaces leading to $|C|$ being larger than unity. This results in the Eulerian scalar derivatives (following a fluid particle) to be larger than ones in Lagrangian coordinates. The length scale of variation of C_{ia} is likely to be of the order of the characteristic length scale of the small scales which cause the strecthing or shrinking. This scale is the Kolmogorov length scale, η. In the absence of reaction, the length scale of variation of the Lagrangian scalar derivatives will depend largely on the initial length scale of the scalar field. It was argued in M Girimaji (1992c) that, if the Kolmogorov length scale is of a different order of magnitude than the initial length scale of the scalar field then, C_{ia} and the Lagrangian scalar derivatives would be poorly correlated.

Chemical reaction can cause the Eulerian scalar derivatives to be different from those in inert mixing. It is important to evaluate the validity of the poor-correlation simplification in the reacting case. In the *distributed regime* of turbulent combustion (Damköhler number smaller than unity), the reaction zone (flame thickness) is larger than the Kolmogorov length scale. It is unlikely that chemical reaction can cause the scalar derivatives to be significantly different from the inert-mixing case. As a result, as in the case of inert mixing, the Lagrangian scalar derivatives would be poorly correlated with C_{ia}. In the *flamelet regime* of turbulent combustion (Damköhler number greater than unity), the flame thickness is smaller than the Kolmogorov length scale. Infact, at the limit of infinite Damköhler number, the reaction zone can be infinitesimally small, causing a discontinuity in the scalar fields. There is no chemical reaction outside these discontinuities. In the reaction zone, it is not clear if the Lagrangian derivative will be poorly correlated with C_{ia}, whereas, outside that zone (regions of no reaction) the poor-correlation simplification is as valid as in the inert-mixing case. Inside the reaction zone the chemical source term is dominant and the molecular diffusion term– and hence its modeling– is unimportant. With increasing Damköhler number – decreasing flame thickness – the volume of the flow field over which the simplification is valid increases and the importance of the diffusion term inside the reaction zone diminishes further. In the limit of Damköhler number going to infinity, the simplification is valid almost everywhere in the flow field except at the inifinitesimally thin flame sheet where the molecular term is insignificantly small. As a result, the poor-correlation simplification should yield reasonable

results even in the flamelet regime of combustion, especially at large Damköhler number. Hence, the expression for the conditional diffusion can be simplified as

$$\Theta_{\phi\alpha} = \langle \frac{\partial x_a}{\partial X_i} \frac{\partial x_b}{\partial X_i} \frac{\partial}{\partial x_a} [\rho D_\alpha \frac{\partial \phi_\alpha}{\partial x_b}] | h^T, \underline{\phi} \rangle \approx \langle \frac{\partial x_a}{\partial X_i} \frac{\partial x_b}{\partial X_i} \rangle \langle \frac{\partial}{\partial x_a} [\rho D_\alpha \frac{\partial \phi_\alpha}{\partial x_b}] | h^T, \underline{\phi} \rangle. \tag{12}$$

The quantity $\langle \frac{\partial x_a}{\partial X_i} \frac{\partial x_b}{\partial X_i} \rangle$ is a second-order tensor which, if the turbulent field is isotropic, can be written as

$$\langle \frac{\partial x_a}{\partial X_i} \frac{\partial x_b}{\partial X_i} \rangle = \langle S(t) \rangle \delta_{ab} \tag{13}$$

where $S(t) = \frac{1}{3} \frac{\partial x_a}{\partial X_i} \frac{\partial x_a}{\partial X_i}$. Hence the model for $\Theta_{\phi\alpha}$ is

$$\Theta_{\phi\alpha}(T, \underline{\phi}) = \langle S(t) \rangle \langle \frac{\partial}{\partial x_a} [D_\alpha \frac{\partial \phi_\alpha}{\partial x_a}] | h^T, \underline{\phi} \rangle. \tag{14}$$

Using similar arguments the model for Θ_T can be derived:

$$\Theta_T = \langle S(t) \rangle \langle \frac{\partial}{\partial x_a} [\lambda \frac{\partial T}{\partial x_a} + \sum_{\alpha=1}^{n} \rho h_\alpha^T D_\alpha \frac{\partial \phi_\alpha}{\partial x_a}] | h^T, \underline{\phi} \rangle, \tag{15}$$

The model. Based on the Lagrangian frame analysis, it is proposed that conditional diffusion be modeled by

$$\Theta_T = \langle S(t) \rangle \langle \frac{\partial}{\partial x_a} [\lambda \frac{\partial T^m}{\partial x_a} + \sum_{\alpha=1}^{n} \rho h_\alpha^{Tm} D_\alpha \frac{\partial \phi_\alpha^m}{\partial x_a}] | h^{Tm}, \underline{\phi}^m \rangle, \tag{16}$$

and

$$\Theta_{\phi\alpha} = \langle S(t) \rangle \langle \frac{\partial}{\partial x_a} [\rho D_\alpha \frac{\partial \phi_\alpha}{\partial x_a}] | T^m, \underline{\phi}^m \rangle. \tag{17}$$

In the above equation, the superscript m refers to the model variables.

The effect of the velocity field on the scalar evolution in the Lagrangian reference-frame is much smaller than the effect in the Eulerian reference frame. Under the poor-correlation simplification, the scalar field evolution in the Lagrangian frame can be considered independent of the velocity field. Hence, the model variables (h^{Tm} and $\underline{\phi}^m$) can be considered to evolve according to

$$\rho \frac{d\phi_\alpha^m}{dt} = \langle S(t) \rangle \frac{\partial}{\partial x_a} [\rho D_\alpha \frac{\partial \phi_\alpha^m}{\partial x_a}] + w_\alpha(\underline{\phi}^m), \tag{18}$$

and

$$\rho \frac{dh^{Tm}}{dt} = \langle S(t) \rangle \frac{\partial}{\partial x_a} [\lambda \frac{\partial T}{\partial x_a} + \sum_{\alpha=1}^{n} \rho h_\alpha^{Tm} D_\alpha \frac{\partial \phi_\alpha^m}{\partial x_a}] - \sum_{\alpha=1}^{n} h_\alpha^0 w_\alpha(\underline{\phi}^m). \tag{19}$$

6

Equations (18) and (19) have two important uses. First, they form a statistical model of the chemically-reacting flow equations (1) and (2). Second, the model equations are similar enough to the original equations that many of the other scalar mixing models – multiscalar mapping closure models (Pope 1991, Gao and O'Brien 1991, Girimaji (1993)), multivariate β-pdf model, JET model – cannot distinguish the difference between pdf's of the two sets of instantaneous equations. Hence, for validating many statistical aspects of the other models, DNS of equations (18) and (19) can be used rather than the more expensive DNS of turbulent reacting flow equations (1) and (2).

What is $\langle S(t) \rangle$**?** The quantity $\langle S(t) \rangle$ is a measure of the mean deformation of the Eulerian coordinate frame caused by the velocity field and can be interpreted as the diffusion enhancement factor. It can be expressed in terms of the deformation characteristics of a material cube attached to a Lagrangian point $\mathbf{x}$ (Girimaji 1992c):

$$S(\mathbf{x}, t) = \frac{1}{3V^2}[A_1^2(t) + A_2^2(t) + A_3^2(t)], \tag{20}$$

where $A_a(\mathbf{x}, t)$ is the area of surface of the cube which was initially coincident with the a axis and $V(\mathbf{x}, t)$ is the volume of the cube. The initial values are such that,

$$A_1(\mathbf{x}, 0) = A_2(\mathbf{x}, 0) = A_3(\mathbf{x}, 0) = V(\mathbf{x}, 0) = S(\mathbf{x}, 0) = 1.$$

For an incompressible velocity field, the volume $V(\mathbf{x}, t)$, which also represents the density ratio following a fluid particle, is always unity. The compressibility of the velocity field manifests itself on the scalar mixing through V. In an isotropic velocity field, the various area magnitudes (A_1, A_2, and A_3) are all statistically equivalent. Hence, assuming isotropy (and incompressibility)

$$\langle S(t) \rangle = \langle A^2(\mathbf{x}, t) \rangle, \tag{21}$$

where $A(t)$ represents the area at any time t of any typical material-surface element (of initial unit area) associated with the fluid element. Material element deformation in isotropic turbulence was studied by Girimaji and Pope (1990) and its implications on $\langle S(t) \rangle$ is discussed

7

in detail by Girimaji (1992c). It suffices to say here that in isotropic turbulence $\langle S(t) \rangle$ grows in time nearly exponentially. The logarithmic growth rate is approximately

$$p(t) \equiv \frac{d \ln \langle S \rangle}{dt} \approx \frac{0.8}{\tau_\eta}, \tag{22}$$

where τ_η is the Kolmogorov time scale of the turbulence. The diffusion enhancement factor $\langle S(t) \rangle$ reflects the cascading effect of the velocity field on the scalar field. As the scalar energy cascades from large scales to small scales, the Eulerian scalar gradient following a fluid element increases exponentially. The diffusion enhancement effect of the velocity field is more prominent at later times when more of the scalar energy is in the small scales.

3   Further simplification and simulation

We want to consider the simplest non-trivial case of multiscalar mixing and combustion where reaction affects the evolution of scalar pdf. For this purpose, several previous authors (e.g., Pope 1991) have used the following set of equations:

$$\frac{\partial \phi_\alpha}{\partial t} + U_i \frac{\partial \phi_\alpha}{\partial X_i} = D_\alpha \frac{\partial^2 \phi_\alpha}{\partial X_i \partial X_i} + w_\alpha. \tag{23}$$

The above equation represents constant-density, isothermal chemical reactions between scalars of different, but, constant diffusivities. If the velocity field $\mathbf{U}$ is isotropic, the enhanced-diffusion reaction model corresponding to equation (23) is

$$\frac{d\phi_\alpha^m}{dt} = \langle S(t) \rangle D_\alpha \frac{\partial^2 \phi_\alpha^m}{\partial x_a \partial x_a} + w_\alpha(\underline{\phi}^m). \tag{24}$$

The time-dependent diffusion enhancement factor is calculated from equation (22).

We consider reversible reactions of the type

$$A + B \leftrightarrow 2P, \tag{25}$$

where, scalars A and B are reactants and scalar P is the product. The factor two is included in equation (25) to conserve mole fractions. The chemical production rate of the three species are

$$w_A = -k_f \phi_A \phi_B + k_b \phi_c^2 \tag{26}$$

$$w_B = -k_f \phi_A \phi_B + k_b \phi_c^2$$

$$w_P = 2k_f \phi_A \phi_B - 2k_b \phi_c^2,$$

where, k_f and k_b are the forward and the backward reaction-rate coefficients. The backward coefficient is usually expressed in terms of the forward rate: $k_b = k_e k_f$, where k_e is the equilibirium constant.

3.1   Simulations

The problem of non-premixed, randomly and isotropically distributed scalars undergoing enhanced mixing and chemical reaction is considered. Numerical simulations of equation (24) are performed in a cubical domain with periodic boundary conditions. A pseudo-spectral method is used: the scalar spatial derivatives are sought in spectral space, whereas, the reaction-rate term is calculated in physical space. The initial scalar field is specified in the manner described in Girimaji (1993). The initial scalar field has a prescribed length scale l_ϕ, and the initial joint pdf, $F(\phi_A, \phi_B)$, is given by

$$F(\phi_A, \phi_B; 0) = \mu_A(0)\delta(\phi_A - 1)\delta(\phi_B) + \mu_B(0)\delta(\phi_A)\delta(\phi_B - 1) + \mu_P(0)\delta(\phi_A)\delta(\phi_B). \quad (27)$$

In the above equation, μ_A, μ_B and μ_P represent the means of species A, B and P respectively. The mass fraction of P is given by

$$\phi_P = 1 - \phi_A - \phi_B. \quad (28)$$

Even when the scalar field evolution is governed by the simple enhanced-diffusion reaction system (equations 24 and 26), the scalar joint-pdf evolution is affected by several parameters: i)τ_η (the Reynolds number); ii) l_ϕ (initial length scale of the scalar field); iii) D_A, D_B (Prandtl number and relative diffusion); iv) μ_A, μ_B (stoichiometric ratio); v) k_f (Damköhler number); and, vi) k_b (reversibility). In this study, we fix the values of τ_η (corresponding to a Taylor-scale Reynolds number of approximately 60, as reported in Girimaji and Pope 1990). The simulations are divided into four groups based on the initial joint pdf. Within each group several simulations are performed by varying the other parameters. The values of the parameters for the various simulations are shown in Table 1.

9

4 Results and implications to turbulent combustion modeling

The results of the simulations are presented in two parts. First, the effect of reaction on the evolution of the means, variances, pdf's and other quantities of interest are studied. Secondly, the simulation data are used in its role as the facsimilie of DNS to evaluate two models of turbulent combustion: the mapping closure model and the assumed β-pdf model.

The effect of chemical reaction on the following statistics of various species are examined:

1. The mean, variances and correlations.

2. The evolution of the pdf.

3. The mean scalar dissipation and chemical production rate of variance.

4. The evolution of the conditional scalar dissipation.

Results from the simulations of Group 1 and Group 2 are used in this part of the study. Statistics of species A and P only are presented, since ϕ_B can be completely determined knowing ϕ_A and ϕ_P. In the discussions below, angular brackets imply mean and primes denote fluctating part of a random variable.

Means. The mean evolutions for Groups 1 and 2 are presented in Figures 1 and 2 respectively. As is to be expected, the means do not change for the inert cases: $\langle \phi_A \rangle$ remains at its initial value, and $\langle \phi_P \rangle$ is always zero. As for the reacting cases, the mean reactant decreases more rapidly for larger k_f (reaction rate coefficient) than for smaller k_f. In the reversible reaction cases (C1b and C2b), the mean values asymptote to equlibrium values given by the equation

$$\mu_A \mu_B = \mu_P^2. \tag{29}$$

The above equation in conjunction with equation (28) leads to the following equlibrium values: for case C1b, $\mu_A = 0.33$, $\mu_B = 0.33$, $\mu_P = 0.33$; and for case C2b, $\mu_A = 0.116$, $\mu_B = 0.616$, $\mu_P = 0.267$.

Variances. The evolution of variance in reacting field in given by

$$\frac{d\sigma_\alpha^2}{dt} = 2(-\epsilon_\alpha^d + \epsilon_\alpha^r), \tag{30}$$

where, the mean scalar dissipation (ϵ_α^d) and the production/destruction of variance due to reaction (ϵ_α^r) are defined as

$$\epsilon_\alpha^d = \langle \frac{\partial \phi_\alpha'}{\partial X_i} \frac{\partial \phi_\alpha'}{\partial X_i} \rangle, \tag{31}$$

$$\epsilon_\alpha^r = \langle w_\alpha' \phi_\alpha' \rangle. \tag{32}$$

The variances of species A for Groups 1 and 2 are shown in Figures 3 and 4. In Group 1, reaction appears to cause the variance to decay slowly compared to the inert case. On the contrary, in Group 2, the variance decays more rapidly with reaction than without. The effect of reaction on Group 2 is larger than that on Group 1. The reasons for these observations are explained further below, when the behavior of ϵ_A^r is discussed. Although discernable, the magnitude of the modification due to reaction is small enough to be unimportant for practical problems. As shown in Figures 6 and 7, $\epsilon_A^d \gg \epsilon_A^r$ for the cases considered resulting in only a slight modification of the variance evolution.

The variance of the product is initially zero. It grows in time initially, due to the chemical production term; more rapidly in Group 2 than in Group 1. After attaining a peak value, it diminishes due to effect of molecular action.

Correlation between ϕ_A and ϕ_B. The correlation coefficient between species A and B,

$$C_{AB} = \frac{\langle \phi_A' \phi_B' \rangle}{\sqrt{\sigma_A^2 \sigma_B^2}}, \tag{33}$$

is given in Figure 5 for the inert cases C2 and C4 and their reacting counterparts C2b and C4b. At early times, when chemical conversion is small, correlation is not affected much by chemical reaction. With time the correlation for the reacting cases deviate from their inert counterparts, going to lower magnitudes while still preserving a negative sign. The deviation, however, is not too large.

11

Scalar pdf. In order to examine the effect of reaction on the scalar pdf evolution, the pdf of scalar A is plotted in Figure 6 for cases C1 and C1b. Figure 7 contains pdf's of scalar A for cases C2 and C2b. Initially, chemical reaction does not affect the pdf much, for, given the segregated initial condition, molecular mixing should occur first before chemical conversion. However, at later stages, as chemical conversion becomes prevalent, the pdfs are strongly affected. The pdf's develop positive skewness due to chemical depletion, and in both cases tend to δ-functions at zero at long times.

The pdf of the product, scalar P, is plotted in Figure 8 (Cases C1a and C1b) and Figure 9 (Cases C2a and C2b). The pdf's of both groups display bimodal behavior initially. One mode of high probability is at zero value of mass fraction, representing parts of the field containing unmixed reactants. The second mode of high probability is close to the maximum value of mass fraction at that time. With time, the mode at zero disappears, and the other mode migrates to higher values retaining its spike-like form, in cases C1a and C1b. The asymptotic state of the pdf for Group 1 is a δ-function at unity, representing a complete conversion of all reactants to products. In cases C2a and C2b also the mode at zero dissipates with time. The pdf migrates to the right and has wider support (larger variance) unlike C1a and C1b. The asymptotic form of the pdf in these cases (Group 2) is a δ-function at $\phi_P = 0.5$.

Chemical production-rate of variance. The chemical production-rate of variance of species A is given by

$$\epsilon_A^r = \langle w_A' \phi'_A \rangle = -\langle \phi_A \rangle \langle \phi_A' \phi_B' \rangle - \langle \phi_B \rangle \langle \phi_A' \phi_A' \rangle - \langle \phi_A' \phi_A' \phi_B' \rangle. \tag{34}$$

For Groups 1 and 2, the correlation between A and B is nearly negative unity leading to

$$\phi_A' \approx -\phi_B', \tag{35}$$

which when substituted in equation (34) leads to

$$\epsilon_A^r = \langle w_A' \phi'_A \rangle \approx [\langle \phi_A \rangle - \langle \phi_B \rangle]\langle \phi_A' \phi_A' \rangle + \langle \phi_A'^3 \rangle. \tag{36}$$

Similar arguments lead to

$$\epsilon_B^r = \langle w_B' \phi'_B \rangle \approx [\langle \phi_B \rangle - \langle \phi_A \rangle]\langle \phi_B' \phi_B' \rangle + \langle \phi_B'^3 \rangle. \tag{37}$$

12

In Figures 10 and 11, ϵ_A^r of Groups 1 and 2 are presented. The behavior of ϵ_A^r in the two groups can be understood by recalling that for Group 1, $\langle phi_A \rangle = \langle \phi_B \rangle$ and for Group 2, $\langle \phi_B \rangle = \langle \phi_A \rangle + 0.5$, at all times. This yields

$$\epsilon_A^r \approx \langle \phi_A'^3 \rangle. \tag{38}$$

for Group 1. As mentioned earlier, the pdf is positively skewed leading to a positive value for ϵ_A^r. For Group 2

$$\epsilon_A^r \approx -0.5\langle phi_A'^2 \rangle + \langle \phi_A'^3 \rangle. \tag{39}$$

For this group, the first term on the right hand side (of equation 39) dominates the skewness term leading to a larger negative value of ϵ_A^r. The behavior of the variances of the two groups is consistent with the above explanations.

Figures 12 and 13 contain ϵ_P^r of groups 1 and 2. Both groups exhibit similar behavior. Starting from zero, the value of ϵ_P^r increases to a peak value and then diminishes to near-zero values. The peak value is higher for higher k_f. The early behavior of ϵ_P^r of the reversible case is identical to its non-reversible counterpart. However, its peak value is not as high, and it diminishes much more rapidly to zero.

Mean scalar dissipation. The mean scalar dissipation of species A of Groups 1 and 2 are given in Figures 10 and 11. Similarly to its effect on variance, reaction causes the mean scalar dissipation to decay more slowly in Group 1 and more rapidly in Group 2. Again, the magnitude of modification is not very large. In both groups, the magnitude of the mean scalar dissipation is much larger than that of chemical production-rate of scalar variance.

The mean scalar dissipation of P of Groups 1 and 2 are given in Figures 12 and 13. In both the groups, with the formation of products, the mean scalar dissipation increases from a zero initial value. After attaining a maximum value, the dissipation decreases. The mean scalar dissipation achieves higher values in Group 2 than the corresponding cases in Group 1. Initially, ϵ_P^r is larger in magnitude than ϵ_P^d, leading to a growth of σ_P^2 from its initial zero value. At latter times, ϵ_P^d is larger leading to a decay in the variance levels. The implication is that initially the scalar-P evolution is reaction controlled, after which both reaction and diffusion are equally important, and ultimately the evolution is diffusion controlled.

13

Conditional scalar dissipation. The evolution of the conditional scalar dissipation of scalar A in cases C2 (inert) and C2b (reacting) is given in Figure 14. Chemical reaction has two effects on this quantity. The first is due to the more rapid decline in the maximum value of ϕ_A as a result of reaction. The zero of the conditional dissipation migrates with the extremum value (Girimaji 1992b). When mixing is accompanied by reaction, the conditional dissipation is non-zero over a smaller range of ϕ_A, than in the case of inert mixing. This effect is negligible at the early stages and more pronounced in the later stages. The second difference is the higher value of the conditional dissipation (where it is non-zero) at a given value of mass fraction in the reacting case as compared to inert case. Again, this difference is large in the latter stages and negligible in the early part. Despite the higher values of the conditional scalar dissipation in the reacting case than in the inert case, the mean scalar scalar dissipation is indeed lower in the reacting case, as shown in Figure 11. The reason for this is the shift in the pdf (Figure 11) due to reaction. In the reacting case, the high values of conditional dissipation occur at values of mass fraction of low probability of occurence and *vice versa*. Whereas, in the inert case high probability and high conditional dissipation appear to occur at nearly same values of mass fraction.

The conditional scalar dissipation of the product, scalar P, is given in Figure 15 for cases C2a and C2b. The conditional dissipation of the product is very unlike that of the reactant for this case. Initially, it is non-zero over a very narrow range of ϕ_P values and it gradually widens with time (or reaction). The peak value normalized by the mean scalar dissipation decreases with time, indicating gentler gradients in the product field at later times. The behavior of this quantity is further discussed later when the modeling issues are examined.

So far in this section, the effect of reaction on various quantities of interest was examined. It is found that although the mean and pdf of the scalars are strongly affected by reaction, other quantities like the variance (and, perhaps, other even moments) are not very different from their inert-mixing counterparts. Hence, it would be useful to directly compare and evaluate models of inert mixing against the enhanced-diffusion/reaction data.

14

4.1 Models vs. Data

We attempt to answer three specific questions regarding turbulent combustion modeling using other models:

1. Can the inert mixing multiscalar mapping-closure model (Girimaji 1993) be used for reacting flows without modification?

2. How good is the multivariate assumed β-pdf model (Girimaji 1991a) for calculating reacting flows?

3. How does the computationally simple assumed-pdf model compare with mapping-closure model for multiscalar mixing?

Multiscalar mapping closure model. The multiscalar mapping closure model for inert mixing (Girimaji 1993) is based on the simplification that the conditional scalar diffusion of a given scalar is a function of that scalar only:

$$\Theta_{\phi\alpha} = \langle \frac{\partial}{\partial X_i}[D_\alpha \frac{\partial \phi_\alpha}{\partial X_i}]|T, \underline{\phi} \rangle \approx \langle \frac{\partial}{\partial X_i}[D_\alpha \frac{\partial \phi_\alpha}{\partial X_i}]|T, \phi_\alpha \rangle. \tag{40}$$

The conditional scalar diffusion for each scalar is obtained by employing the mapping closure procedure for single scalar mixing. Knowing the conditional scalar diffusion of each scalar, the joint pdf evolution is solved, and the results are in reasonably good agreement with data.

Even when mixing is accompanied by reaction, it is suggested in Girimaji (1993) that the simplification stated in equation (40) may be valid. In the reacting case, however, the mapping closure procedure even for single scalar is not clear. So it will be useful to know, if the conditional scalar diffusion implied by the mapping closure procedure for inert mixing is adequate for the reacting case also. Conditional scalar diffusion is related to the conditional scalar dissipation according to

$$\Theta_{\phi\alpha} = \frac{1}{F(\phi_\alpha)} \frac{\partial \chi_{\phi\alpha} F(\phi_\alpha)}{\partial \phi_\alpha}. \tag{41}$$

The inert case mapping closure model (with Gaussian reference field) for conditional scalar dissipation for initially non-premixed reactants is (Girimaji 1992b)

$$\frac{\chi(\phi)}{\chi(0.5)} = exp(-2[erf^{-1}\{2\phi - 1\}]^2). \tag{42}$$

15

This model is quite good in the early stages of inert mixing and is technically invalid but still adequate during the latter stages. The validity of the above model for the reacting case is now investigated.

Shown in Figure 16, are $F(\phi_A)\chi(\phi_A)/\chi(\phi_A = 0.5)$ of the data and model for case C2b. In the model calculation of the above quantity, pdf F is taken from the data. The model agrees with the data very well at early times. At later times, the model is still adequate. Recall that even for the case of inert mixing the model is not very good at the final stages. Perhaps, an inert-case model which is uniformly valid at all times would be good for reacting case at all times too. In any event, for combustion applications, the behavior of the model at the early stages, when the unmixedness is high, is more important than at the late stages when the scalars are more or less uniformly mixed. Hence, for the reactants a closure model for the conditional scalar diffusion obtained by substituting equation (42) in equation (41) might be adequate.

Modeling the conditional diffusion of the product (scalar P) is not as simple. The relative importance of chemical conversion and mixing in the scalar pdf evolution (of P) at various times can be surmised from Figure 9 where the mean scalar dissipation and the chemical production rate of variance are compared. Initially, the evolution of the scalar P is dominated by chemical conversion. Molecular diffusion does not play a significant role in the pdf evolution until much later. Therefore, it is important that the model for the conditional diffusion (or dissipation) of the product be accurate at later times; accuracy at early times is not as crucial. Comparison of $F(\phi_P)\chi(\phi_P)/\chi(\phi_P = 0.5)$ for the product is shown Figure 17 for case C2b. The agreement is very poor in the initial stages. At the later stages, it is much better. Whether the model is good enough for engineering applications can be determined only from the computation of the pdf evolution using the closure model. Such a computation is outside the scope of this work.

Assumed multivariate β-pdf model. In the assumed-pdf approach the scalar joint pdf is prescribed knowing the first few moments of the scalar field. It is computationally far less intensive than the mapping closure model and is ideally suited for engineering computations.

16

The assumed multivariate β pdf model for a N-scalar mixing process is given by (Girimaji 1991a)

$$F(\underline{\phi}) = \frac{\Gamma(\beta_1 + \cdots + \beta_N)}{\Gamma(\beta_1)\cdots\Gamma(\beta_N)}\phi_1^{\beta_1-1}\phi_2^{\beta_2-1}\cdots\phi_N^{\beta_N-1}\delta(1 - \phi_1 - \ldots - \phi_N). \qquad (43)$$

The parameters of the model $(\beta_1, \cdots, \beta_N)$ are functions of the mean mass fractions μ_α and turbulent scalar energy Q:

$$\beta_\alpha = \mu_\alpha(\frac{1-S}{Q} - 1). \qquad (44)$$

In the above equation Q and S are given by

$$Q = \sum_{\alpha=1}^{N} \sigma_\alpha^2; \quad S = \sum_{\alpha=1}^{N} \overline{\mu_\alpha}^2. \qquad (45)$$

where σ_α^2 is the variance of mass fraction of scalar α. The above model tested for two-scalar inert mixing process with reasonable success, but is yet to be validated for multiscalar mixing and reaction.

In Figure 18, the individual variances and some cross moments of species A and B calculated using the model are compared against corresponding simulation data for case C1c. Similar comparisons are performed for cases C2c, C3b and C4b in Figures 19, 20 and 21, respectively. The means and the turbulent scalar energy required as inputs to the model are taken from DRS data. The model predicts the variances reasonably well. The magnitude of the cross covariance is consistently underpredicted by the model, but the difference is not too much. For the two higher order cross moments compared ($\langle\phi_A'^2\phi_B'\rangle$ and $\langle\phi_A'\phi_B'^2\rangle$) the model does surprisingly well. For each of the cases considered, the moments behave differently and the model is able to capture the behavior well, qualitatively and quantitatively. Overall the performance of the model is quite satisfactory, given the simplicity of the model.

Multivatiate β-pdf model vs. Mapping closure model. Now the assumed β-pdf model is compared against the more detailed and computationally intensive mapping closure model. The two models are equally good for the case of inert non-premixed two scalar mixing (Girimaji 1992b). Comparison of the two models for multiscalar mixing has not been performed before, and is attempted presently for inert mixing. (As mentioned before, computations of multiscalar reacting flows using mapping-closure model are intensive to be

17

attempted here.) For the purpose of computation, simulations C3 and C4 are used. In the absence of reaction, Groups 1 and 2 reduce to two-scalar mixing, and hence not useful to evaluate multiscalar. In Figure 22, various normalized cross moments (of species A and B) obtained from the simulations are plotted as a function of the variance of scalar A for Case C3. (The variance decreases monotonically in time and hence can be used in lieu of time as the abcissa.) Also shown in the Figure are the cross moments calculated using the two models. The moments of the normalized variables are presented:

$$\theta_\alpha = \frac{\phi_\alpha - \langle \mu_\alpha \rangle}{\sigma_\alpha}. \tag{46}$$

For all the moments considered, both the models agree equally well with the data. Figure 23 presents the same comparison for case C4. In this case, the performance of the mapping closure model is clearly superior. These findings are in keeping with the arguments presented in Girimaji (1991a) that the assumed β-pdf model is likely to be more accurate when the length-scale and diffusivities of the scalars are similar (case C3) than when they are widely disparate (case C4). For case C4, even the mapping closure model is not very accurate. This leads to the question, for engineering calculations, is the increase in accuracy achieved using the mapping closure model worth the extra effort involved in computing? The answer will depend on the application for which the model is being used. In combustion calculations it is the unnormalized moments that appear in the scalar moment equations and need closure modeling, not the normalized moments. Despite the relatively poor agreement of the normalized moments in Figure 23, the unnormalized moments calculated using the β-pdf model are quite close to the data as seen in Figure 21 for the corresponding reacting case C4b. This appears to suggest that the assumed-pdf approach, although simplistic, may be quite adequate for modeling of turbulent combustion in engineering calculations.

5 Conclusion

It is shown that in isotropic turbulence the (enhanced) diffusion-reaction system (18 and 19) can be considered a statistical model of turbulent combustion (equations 1 and 2) with the initial field and the diffusion enhancement factor ($\langle S(t) \rangle$) as inputs. The diffusion-enhancement factor can be found if the scalar variance evolution is known (Girimaji 1992c).

In the event that scalar variance evolution is not known from any other source, a simple model for the diffusion-enhancement factor is provided (equation 22). The enhanced-diffusion reaction model is close enough to the turbulent combustion equations that, in normalized time, many of the other models (mapping closure models, assumed-pdf models and any model that decouples the velocity and scalar fields) cannot distinguish between the present model and the original equations.

Simulations of the diffusion-reaction system is performed in a cubical box (64^3 grid points) from non-premixed initial conditions. The reaction considered is of the type

$$A + B \leftrightarrow P.$$

The reaction is constant-density and cold (isothermal). Several simulations of different initial conditions, reaction-rate coefficient and degree of reversibility are performed (Table 1). The simulations are used to examine the effect of reaction on the evolution of several scalar staistics (Figures 1 - 15). The data are also used to evaluate other models; mapping closure model and the assumed multivariate β-pdf model. The observations and inferences from the study are the following.

1. The conditional scalar dissipation implied by the inert mapping closure model is reasonable even for reacting case but only for the reactants (scalars A and B) as shown in (Figure 16). For the product (scalar P), the agreement is quite poor at early times but better at later times (Figure 17). Since, the evolution of scalar P is initially dominated by chemical conversion and not molecular mixing, the accuracy of the conditional dissipation model at the early stages may not be critical to the overall performance of the model. At the later stages, when the evolution of scalar P is mixing dominated, the model is adequate. For this reason, the use of equations (42 and 41) as closure model may yet yield reasonable results.

2. A close comparison (of the normalized moments) of the multiscalar mapping closure model and the multivariate β-pdf model (Figures 22 and 23) against inert data shows that the two models are quite close when the initial length scales and diffusivities

are similar. The mapping closure model is superior when those parameters are vastly different for the different scalars.

3. The assumed β-pdf model comes reasonably close in calculating many of the unnormalized moments of the scalar joint pdf, even for the reacting case and even when the initial length scale and diffusivities of the participating scalars are quite disparate (Figures 18 - 21). It is the unnormalized moments that require closure modeling in turbulent calculations. Hence, despite the disagreement of the normalized moments under some circumstances, the assumed β-pdf model appears to be adequate for engineering calculations.

References

[1] Chen, H., Chen, S. and Kraichnan, R. H. (1989) *Probability distribution of a stochastically advected scalar field.* Physical Review Letters, **63** (24), 2657 - 2660.

[2] Eswaran, V., and Pope, S. B. (1988) *Direct Numerical Simulations of the turbulent mixing of a passive scalar.* Physics of Fluids, **31** (3), 506 - 520.

[3] Gao, F. (1991) *Mapping closure for multispecies Fickian diffusion.* Phys. Fluids **3** (10), 2438 - 2444.

[4] Girimaji, S. S. and Pope, S. B. (1990) *Material element deformation in isotropic turbulence* J. Fluid. Mech. **220**, pp 427 - 458.

[5] Girimaji, S. S. (1991a) *Assumed β-pdf model for turbulent mixing: validation and extension to multiple scalar mixing.* Combust. Sci. and Tech. **78**, 4 - 6, 177 - 196.

[6] Girimaji, S. S. (1991b) *A simple recipe for modeling reaction rates in flows with turbulent combustion.* AIAA-91-1792. AIAA 22nd Fluid Dynamics, Plasma Dynamics and Lasers Conference, June 24-26, 1991, Honolulu, Hawaii.

[7] Girimaji, S. S. (1992a) *A mapping closure for turbulent scalar mixing using time-evolving reference field.* Phys. Fluids A (in press).

[8] Girimaji, S. S. (1992b) *On the modeling of scalar diffusion in isotropic turbulence.* Phys. Fluids. A, **4** (11), 2529 - 2537.

[9] Girimaji, S. S. (1992c) *Towards understanding turbulent scalar mixing.* NASA Contract. Rep. CR 4446.

[10] Girimaji, S. S. (1993) *A study of multiscalar mixing.* Phys. Fluids. A, **5** (7), 1802 - 1809.

[11] Madnia, C. K., Frankel, S. H., and Givi, P. (1992) *Reactant conversion in homogeneous turbulence: mathematical modeling, computational validations and practical applications.* Theoret. Comput. Fluid Dynamics, **4**, 79 - 93.

[12] Kerstein, A. R. (1988) *A linear eddy model of turbulent scalar transport and mixing.* Combust. Sci. and Tech., **60**, 391 - 421.

[13] Pope, S. B. (1985) *PDF methods for turbulent reacting flows.* Prog. Energy Combust. Sci., **11**, 119 - 192.

[14] Pope, S. B. (1991) *Mapping closures for turbulent mixing and reaction.* Theo. and Comp. Fluid Dynamics, **2**, 255 - 270.

[15] Williams, F. A. (1988) *Combustion Theory.* Addison - Wesley Publishing Company, Inc., New York.
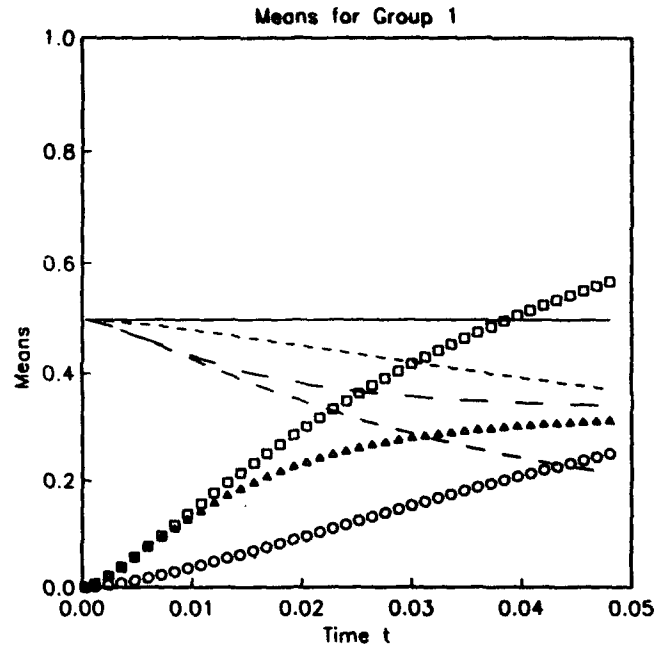
Figure 1: Evolution of the scalar means for Group 1. μ_A : C1 (solid line), C1a (- -), C1b (- -), C1c(— —). μ_P : C1a (circle), C1b (square), c1c(triangle).
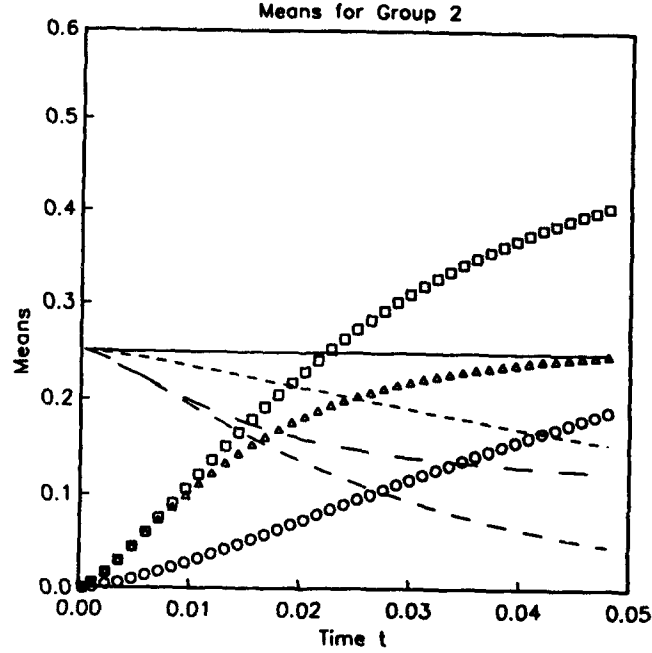
Figure 2: Evolution of the scalar means for Group 2. μ_A : C2 (solid line), C2a (- -), C2b (- -), C2c(— —). μ_P : C2a (circle), C2b (square), c2c(triangle).

22
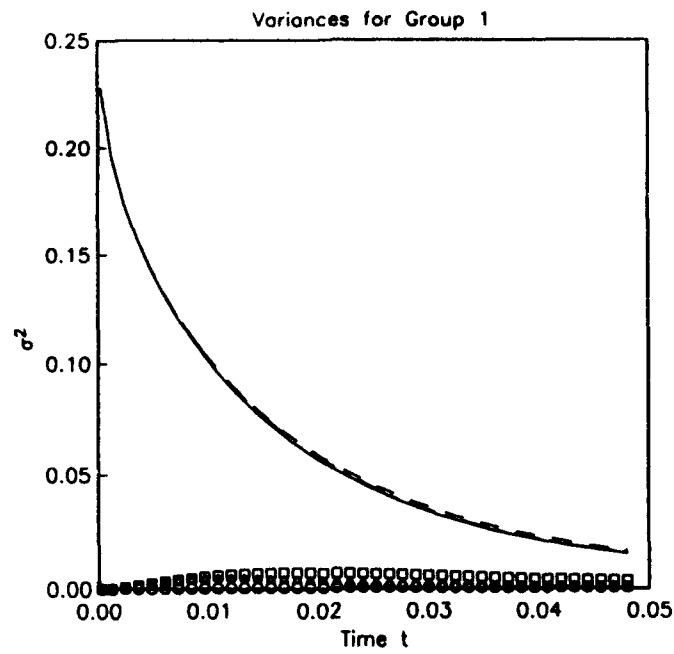
Figure 3: Evolution of the scalar variance for Group 1: Legend same as figure 1
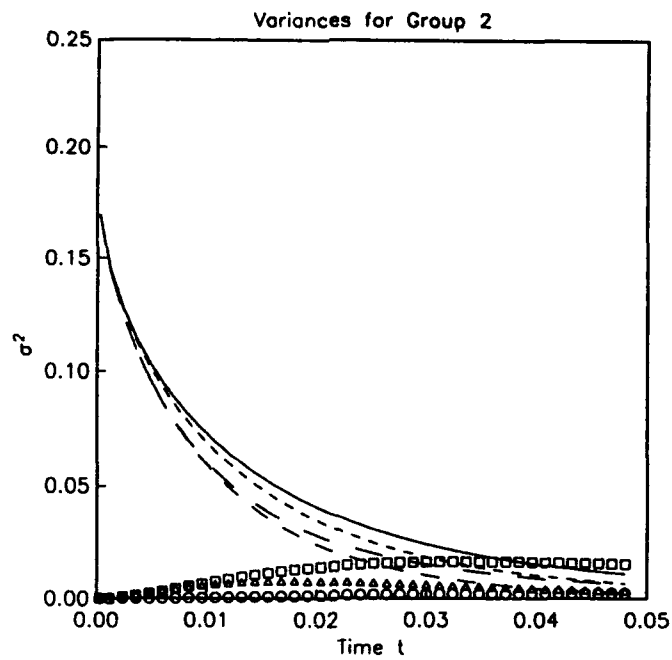
Figure 4: Evolution of the scalar variance for Group 2: Legend same as figure 2.

23
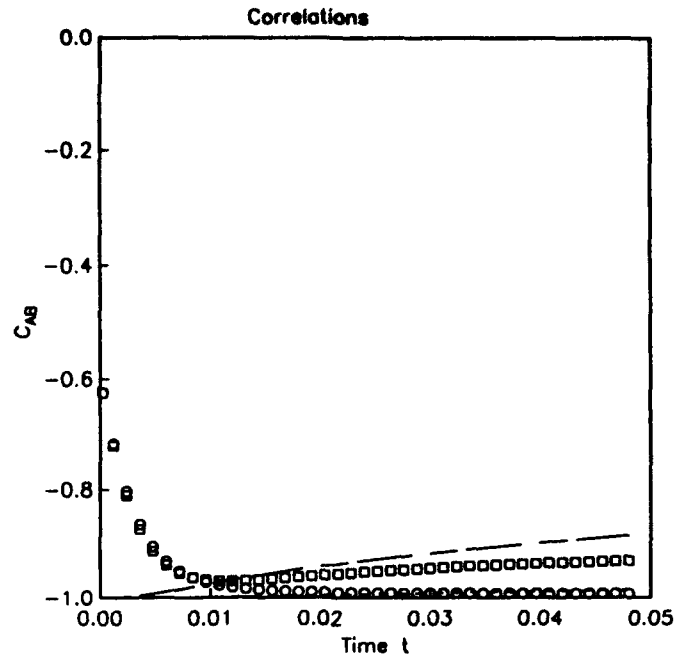
Figure 5: Evolution of the correlation C_{AB}: C2 (- -), C2b (- —), C4 (circle) and C4b (square).
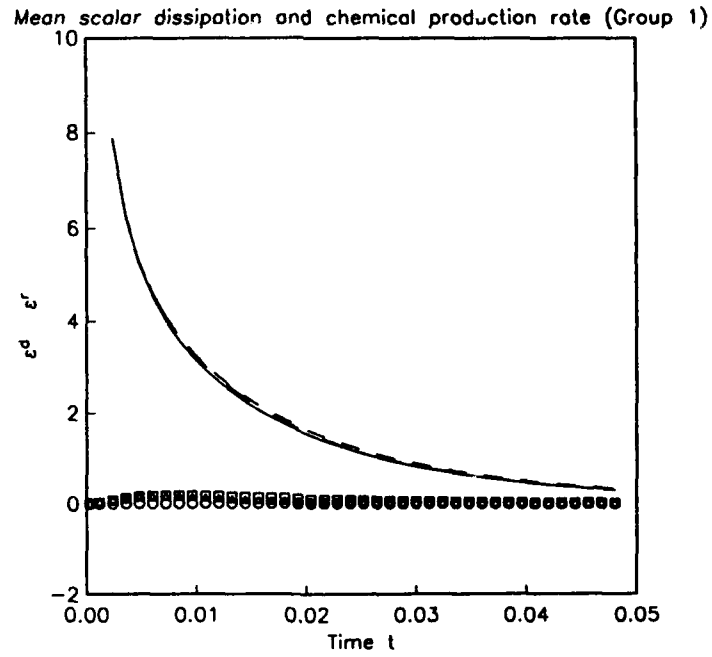
Figure 6: Mean scalar dissipation and chemical production rate of scalar A for Group 1. Mean scalar dissipation : C1 (solid line), C1a (- -), C1b (- -), C1c(— —). Chemical production : C1a (circle), C1b (square), C1c(triangle).

24

Mean scalar dissipation and chemical production rate (Group 2)
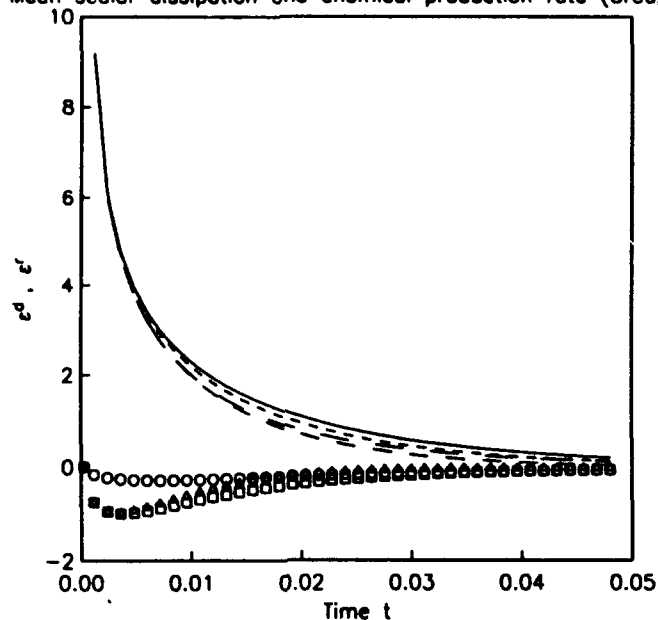
Figure 7: Mean scalar dissipation and chemical production rate of of scalar A for Group 2. Mean scalar dissipation : C2 (solid line), C2a (- -), C2b (- -), C2c(— —). Chemical production : C2a (circle), C2b (square), C2c(triangle).
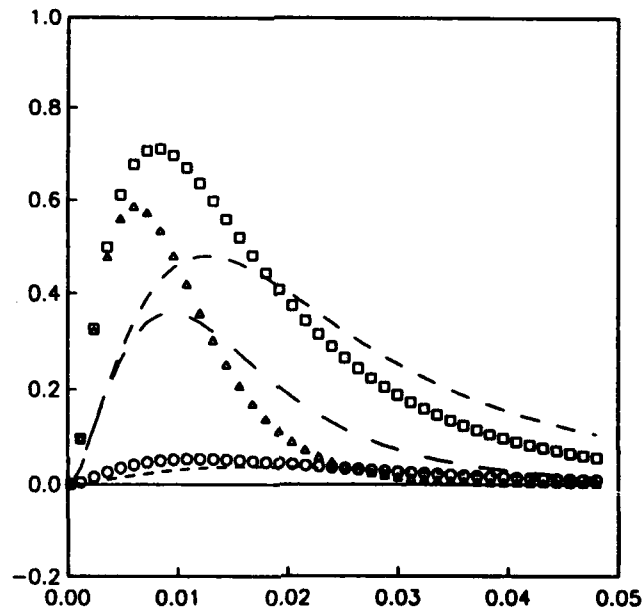
Figure 8: Mean scalar dissipation and chemical production rate of scalar P for Group 1. M^an scalar dissipation : C1 (solid line), C1a (- -), C1b (- -), C1c(— —). Chemical production : C1a (circle), C1b (square), C1c(triangle).

25

Figure 9: Mean scalar dissipation and chemical production rate of of scalar P for Group 2. Mean scalar dissipation : C2 (solid line), C2a (- -), C2b (- -), C2c(— —). Chemical production : C2a (circle), C2b (square), C2c(triangle).
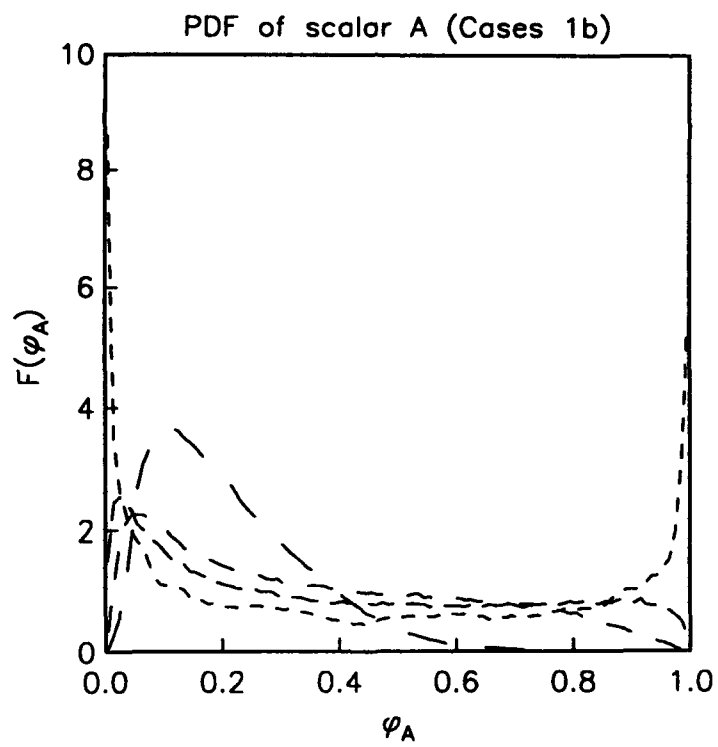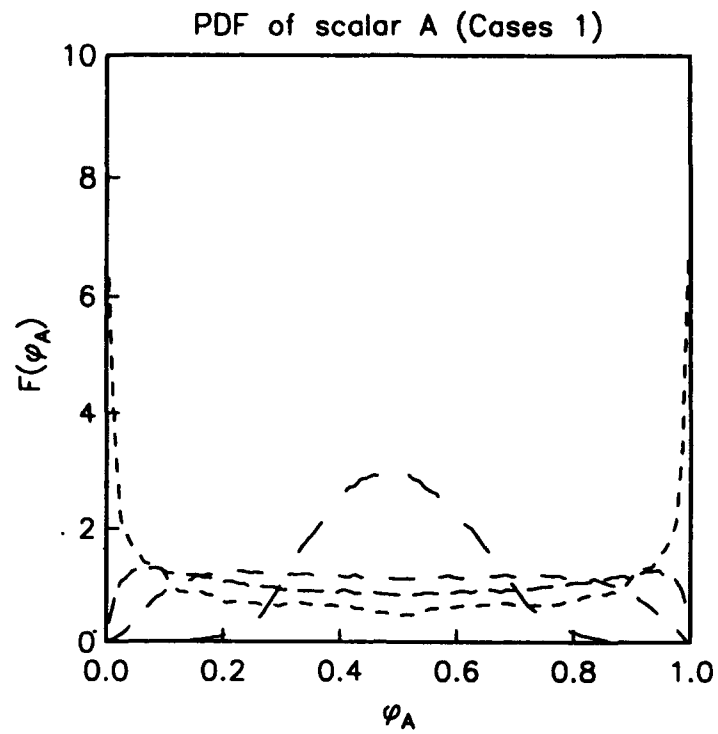
Figure 10: PDF evolution of the scalar A for C1 (a) and C1b (b): Time t = .006 (– –), 0.012 (— —), 0.024 (— —) and 0.048 (— —).
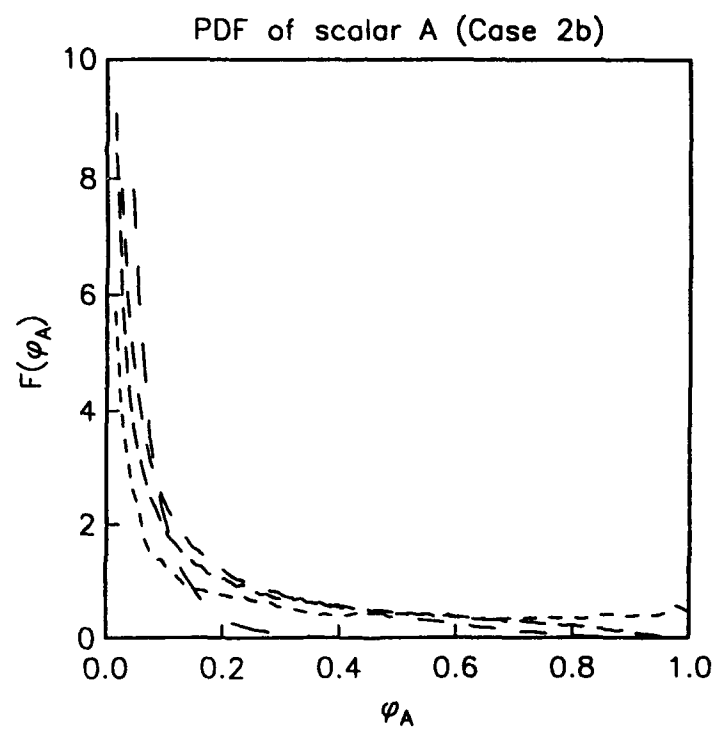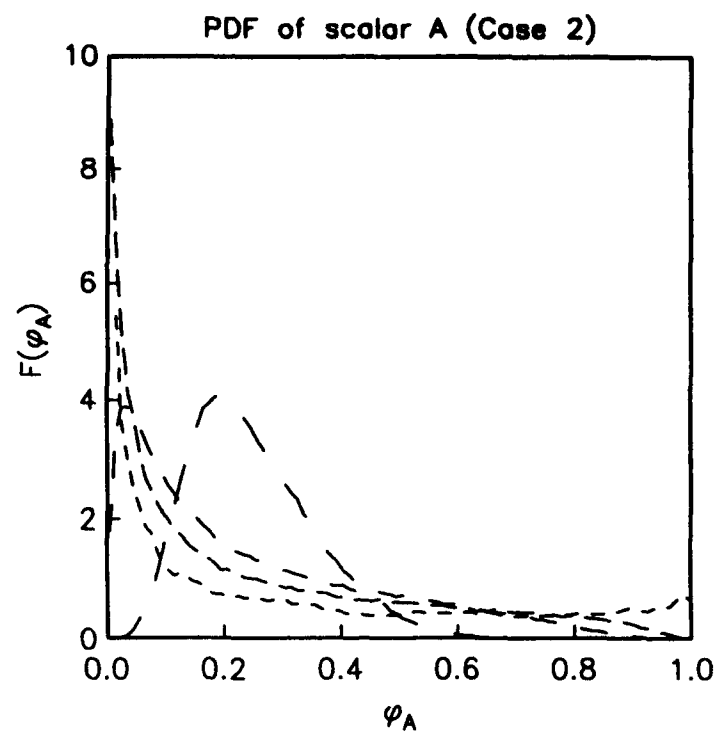
Figure 11: PDF evolution of the scalar A for C2 (a) and C2b (b): Legend same as figure 10.
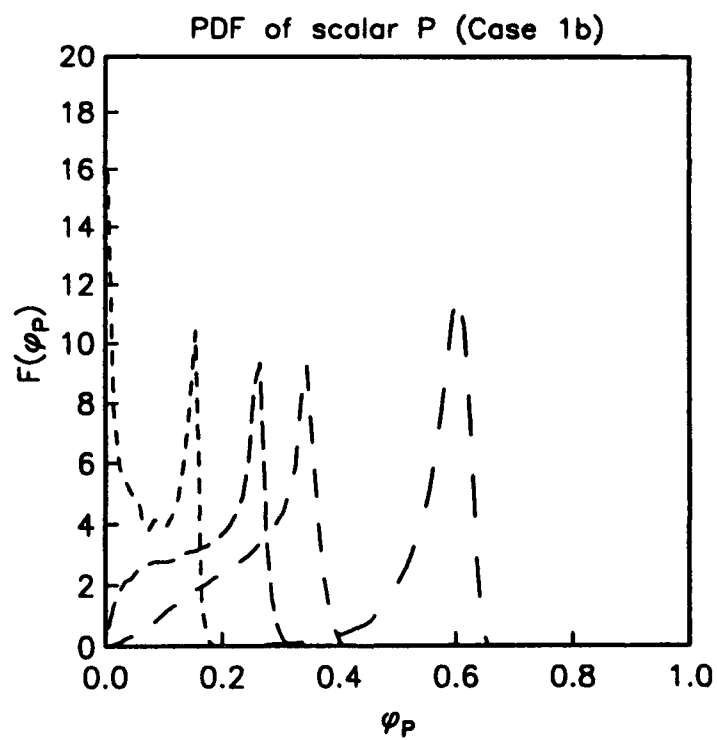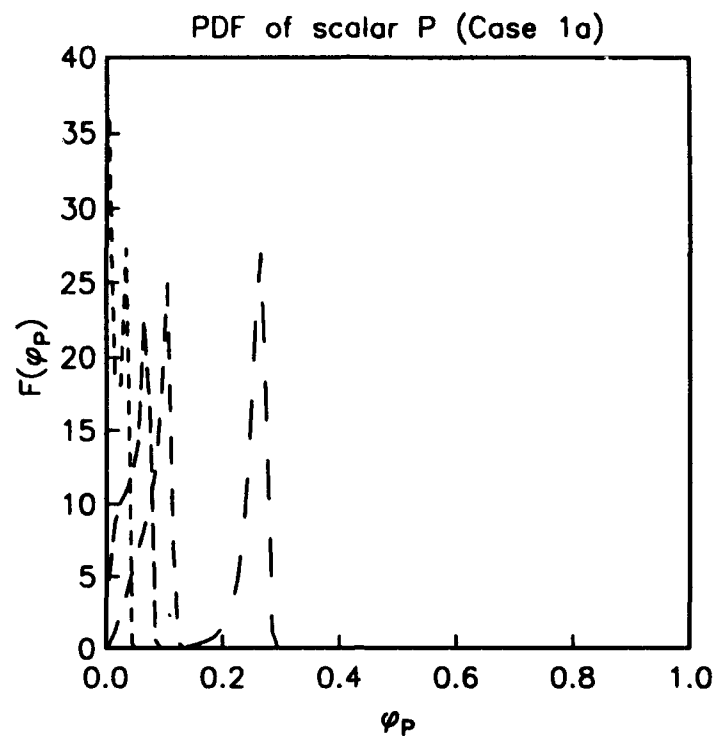
Figure 12: PDF evolution of the scalar P for C1a (a) and C1b (b): Legend same as figure 10.
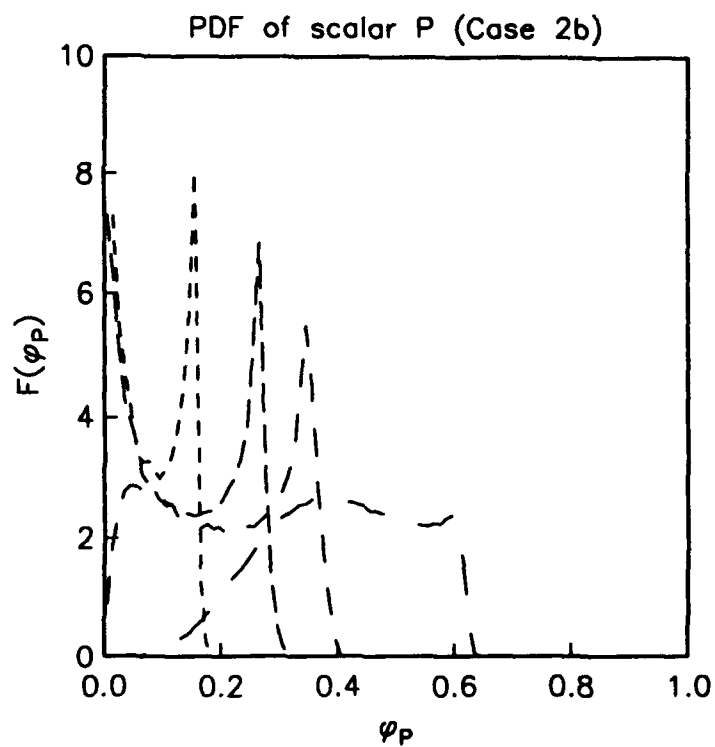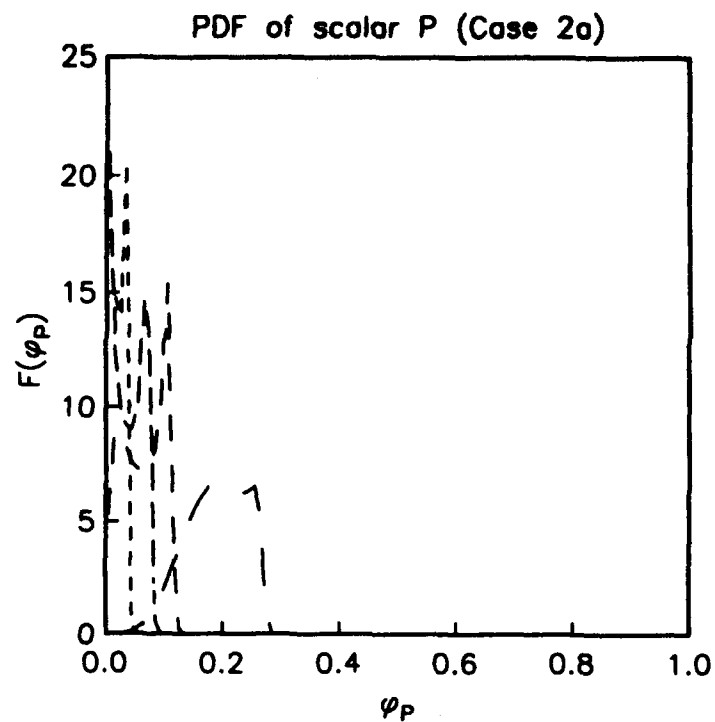
Figure 13: PDF evolution of the scalar P for C2a (a) and C2b (b): Legend same as figure 10.

Conditional scalar dissipation of A (Case 2)

Conditional scalar dissipation of A (Case 2b)
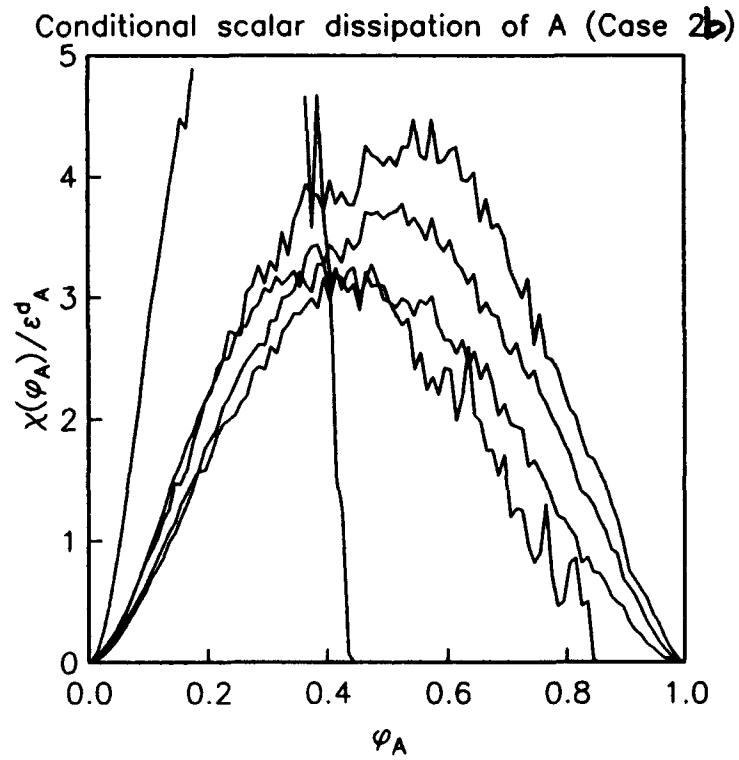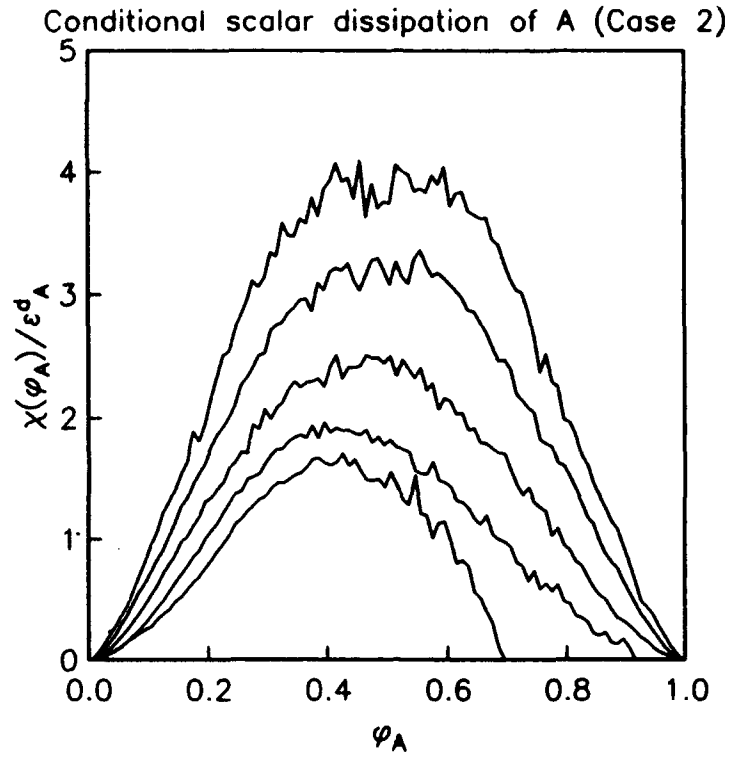
Figure 14: Conditional scalar dissipation of scalar A for C2 (a) and C2b (b): Legend same as figure 10.

31
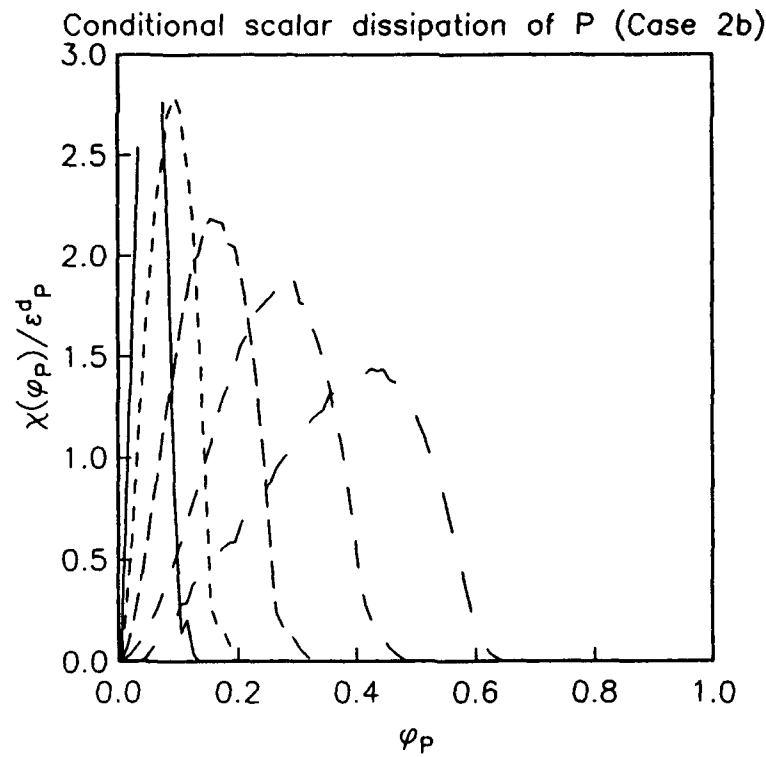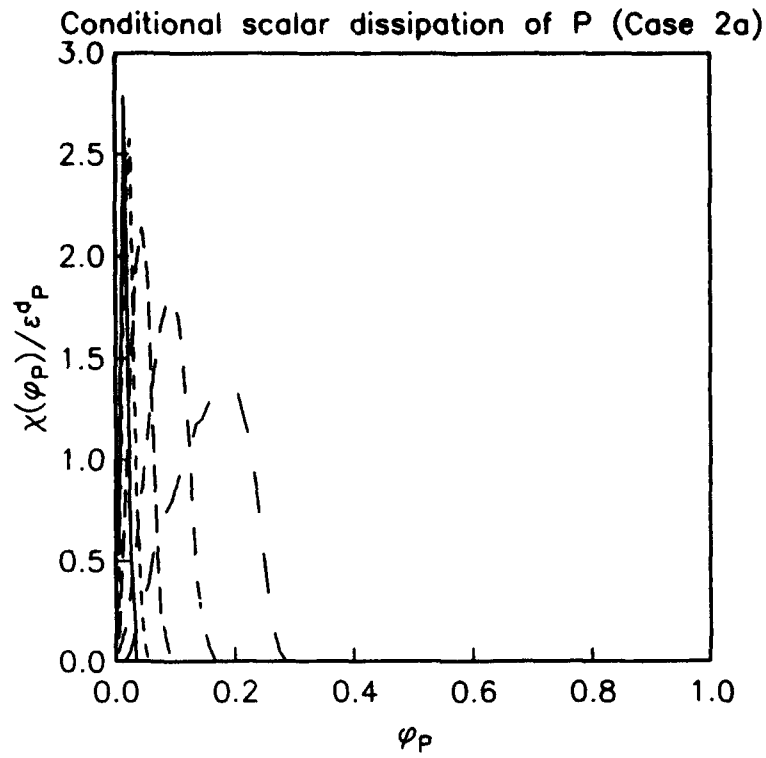
Figure 15: Conditional scalar dissipation of scalar P for C2a (a) and C2b (b): Legend same as figure 10.
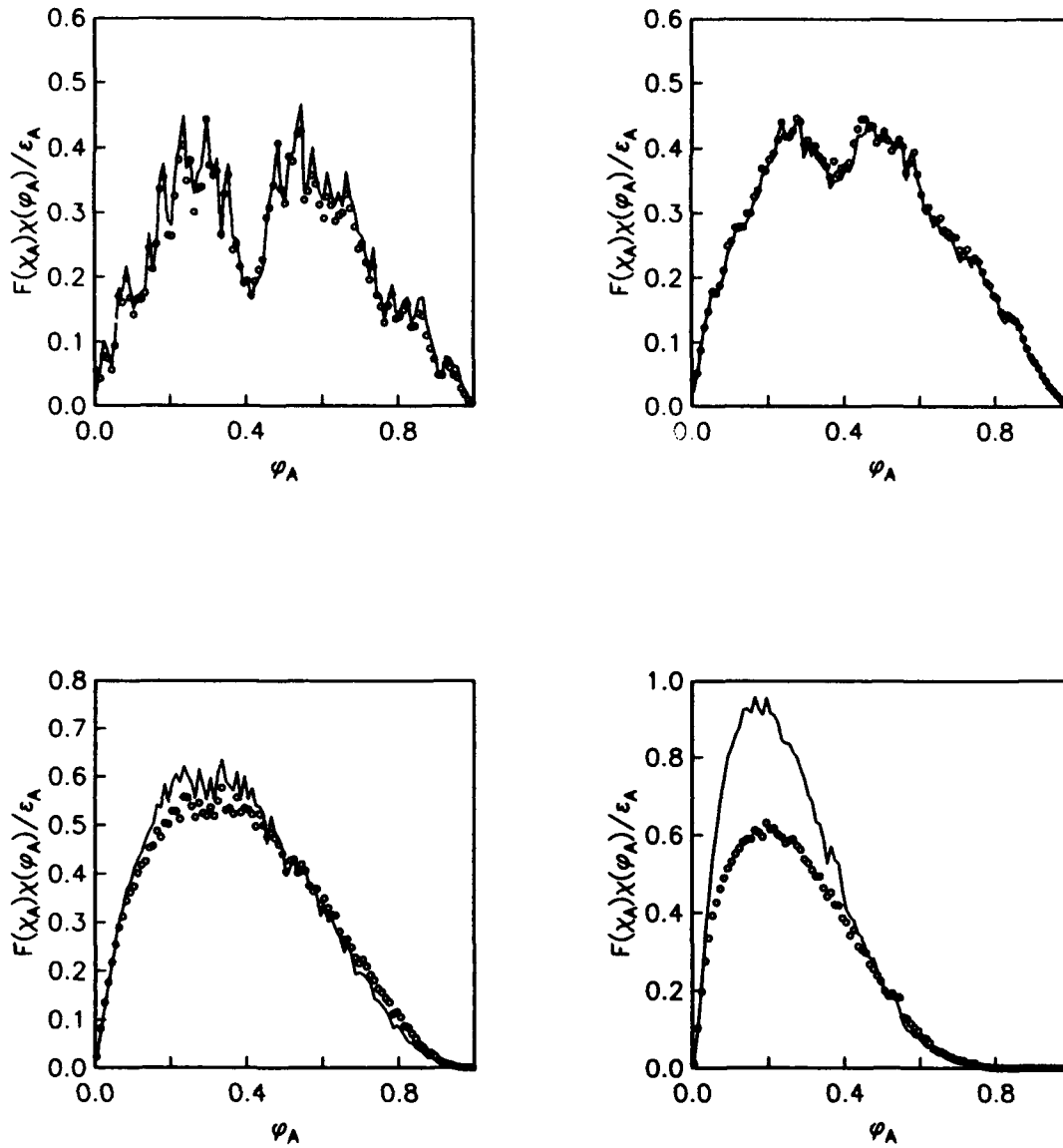
Figure 16: DRS data vs. unmodified mapping closure model. Comparison of $F(\phi_A)\chi(\phi_A)/\epsilon_A$ for Case C2b: Data (solid line), model (circle). (a) t = 0.006, (b) t = 0.012, (c) t = 0.024 and (d) t = 0.048.
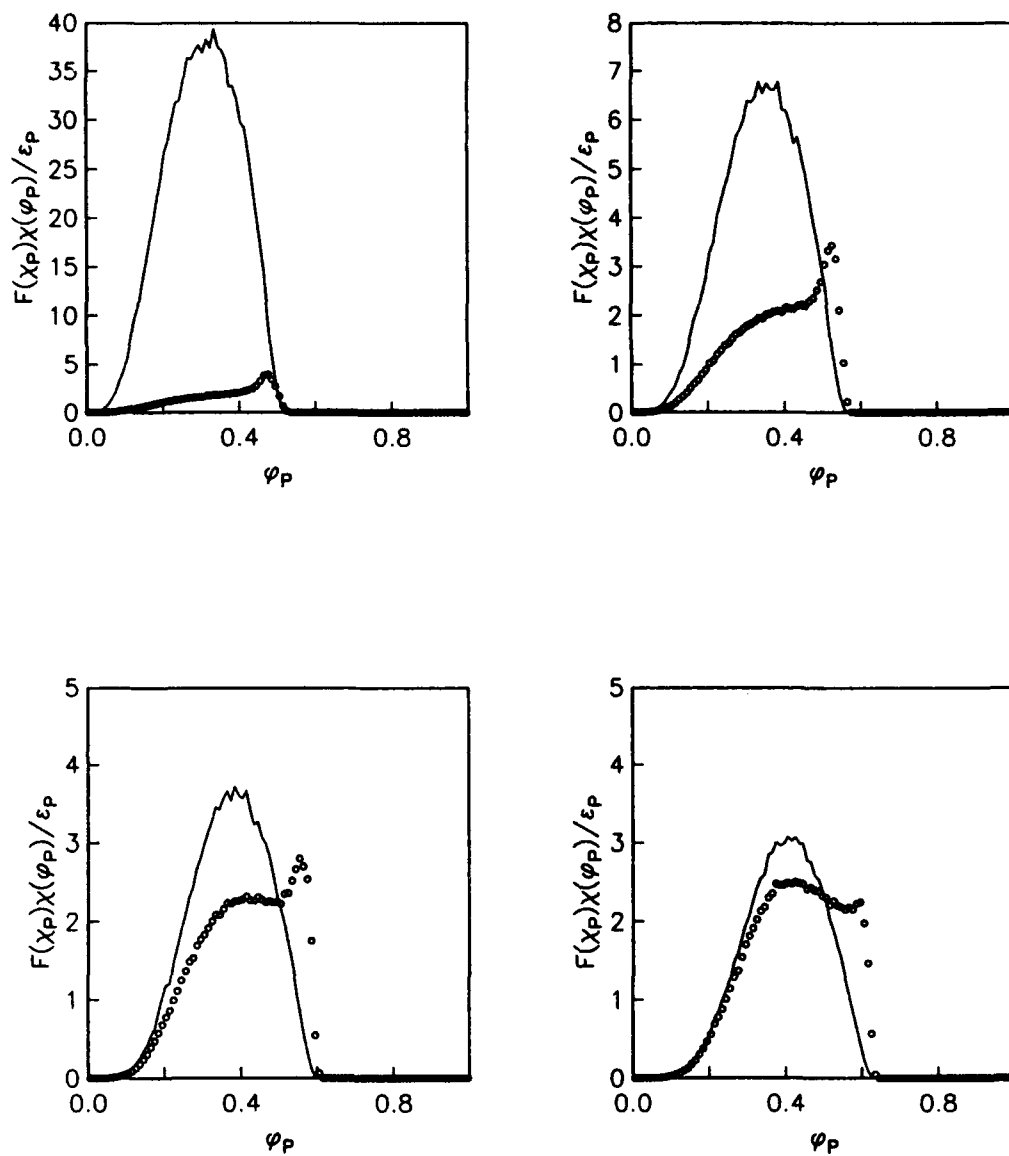
Figure 17: DRS data vs. unmodified mapping closure model. Comparison of $F(\phi_P)\chi(\phi_P)/\epsilon_P$ for Case C2b: Legend same as figure 16.
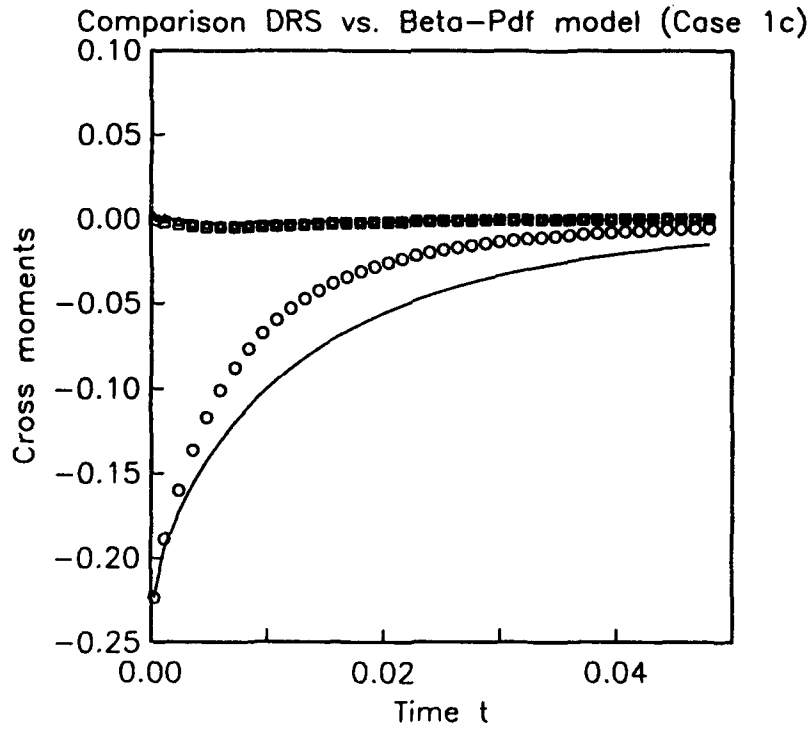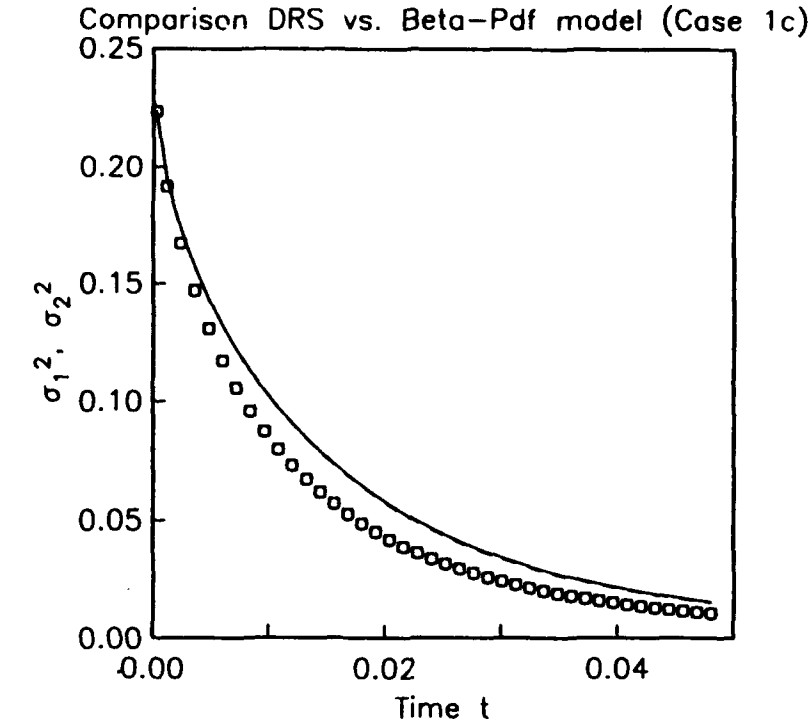
Figure 18: DRS data vs. assumed β-pdf model. Comparison of various unnormalized moments for case C1c. (a) σ_1^2: data (solid line), model (circle); σ_2^2 – data (- -), model (square). (b) $\langle\phi_1\phi_2\rangle$ – data (solid line), model (circle); $\langle\phi_1^2\phi_2\rangle$: data (- -), model (square); and, $\langle\phi_1\phi_2^2\rangle$ – data (— —), model (triangle).
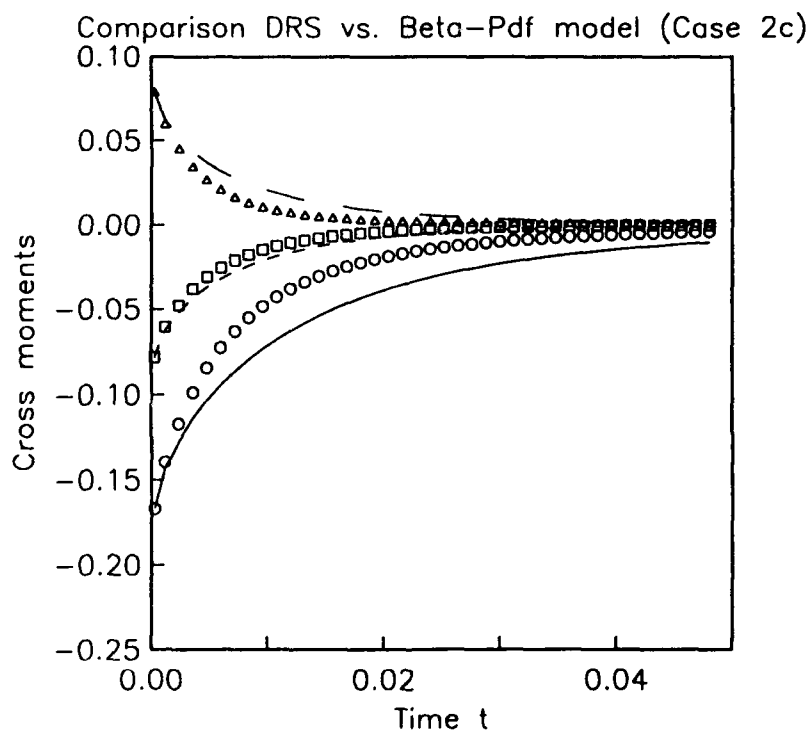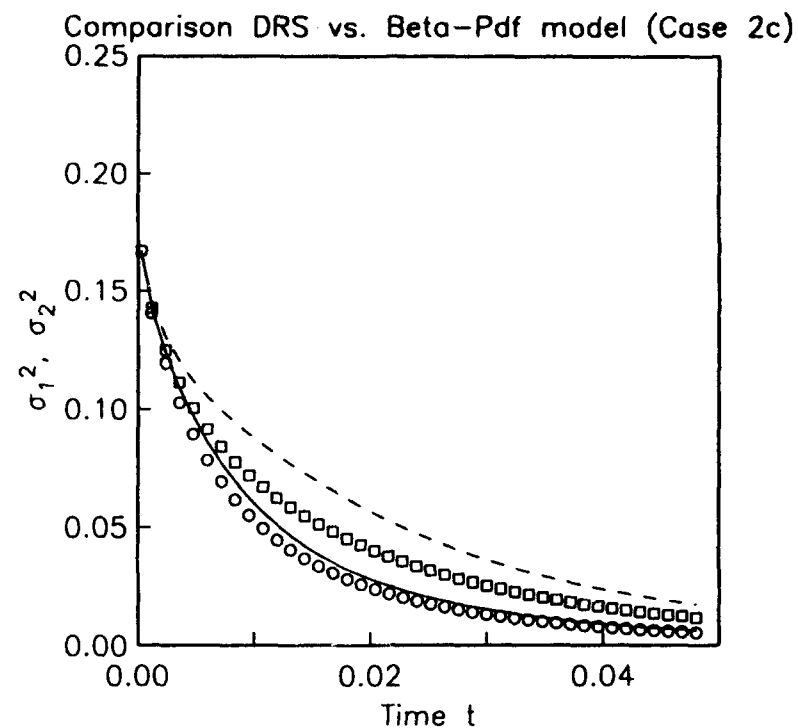
Figure 19: DRS data vs. assumed β-pdf model. Comparison of various unnormalized moments for case C2c. Legend same as figure 18.
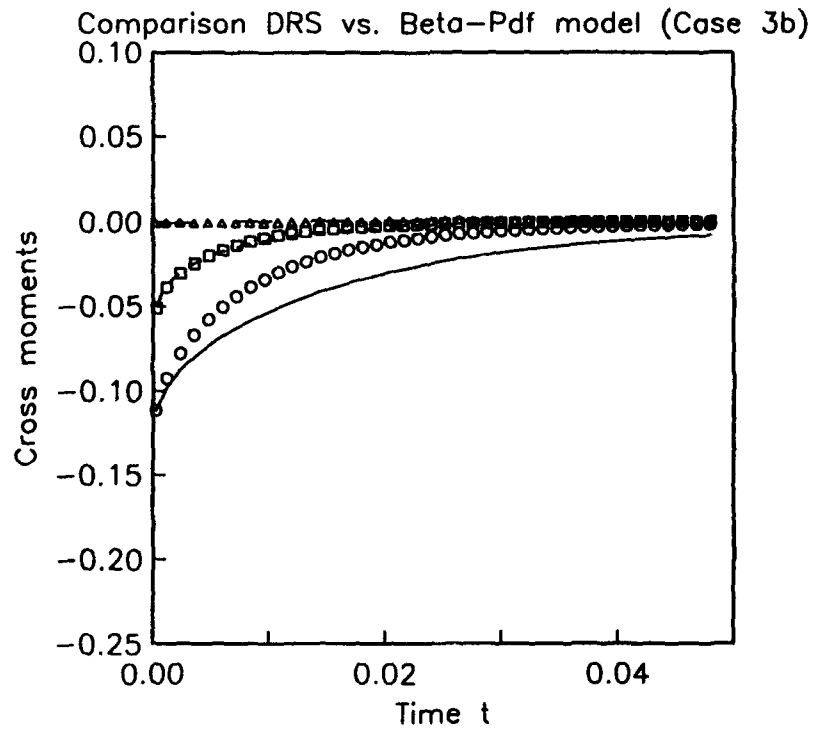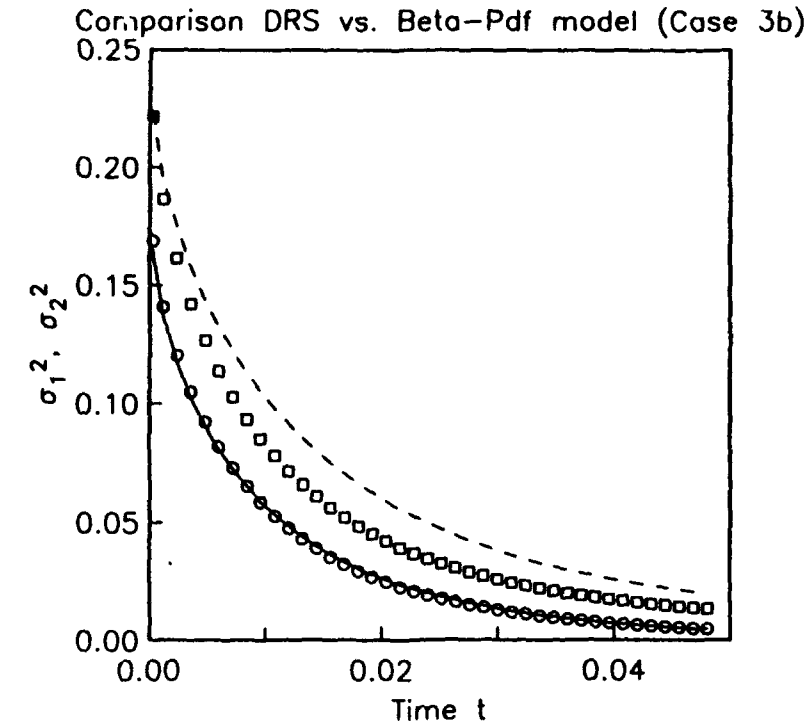
Figure 20: DRS data vs. assumed β-pdf model. Comparison of various unnormalized moments for case C3b. Legend same as figure 18.
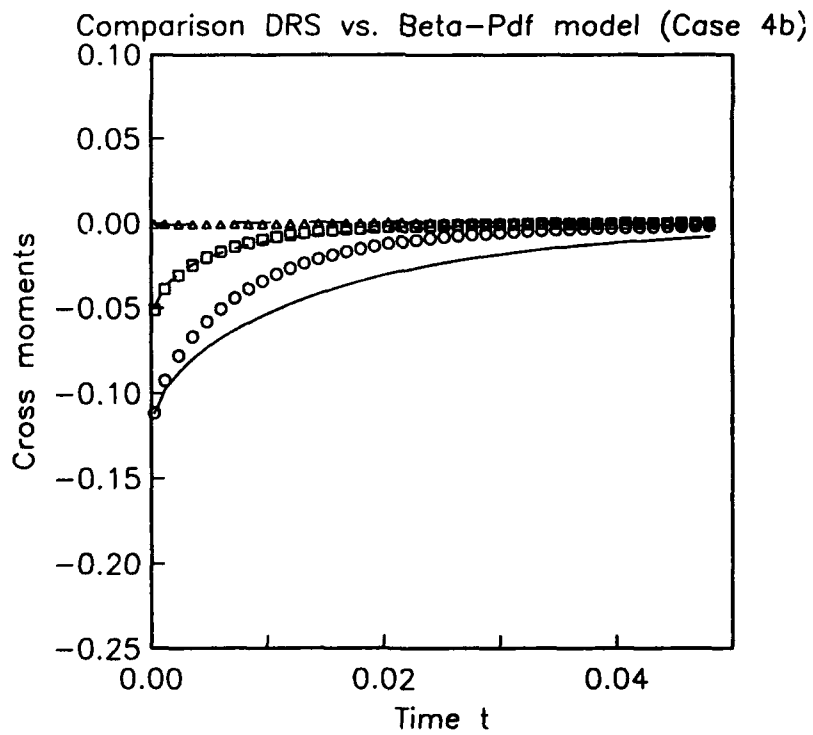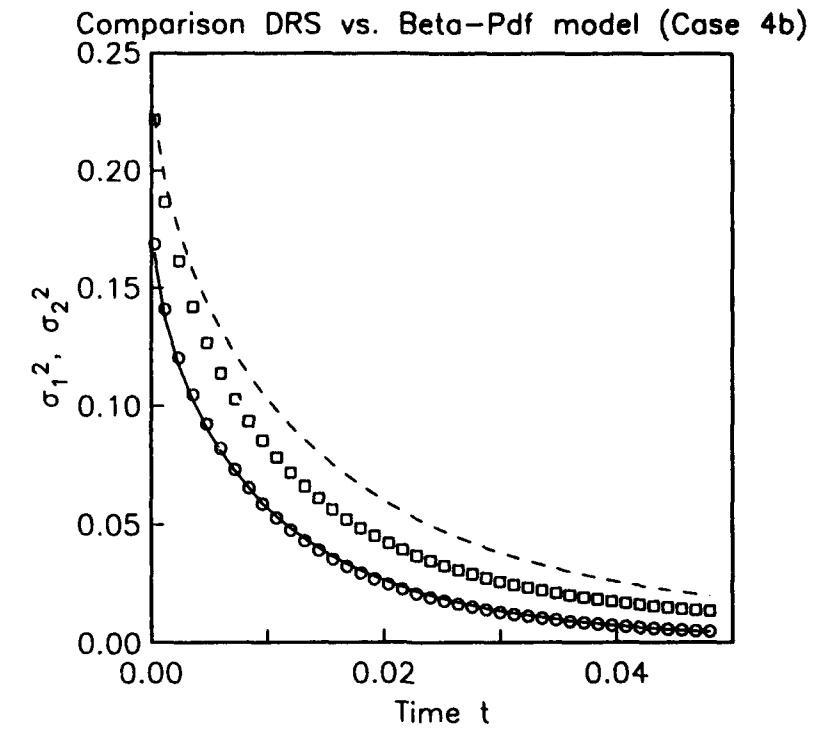
Figure 21: DRS data vs. assumed β-pdf model. Comparison of various unnormalized moments for case C4b. Legend same as figure 18.
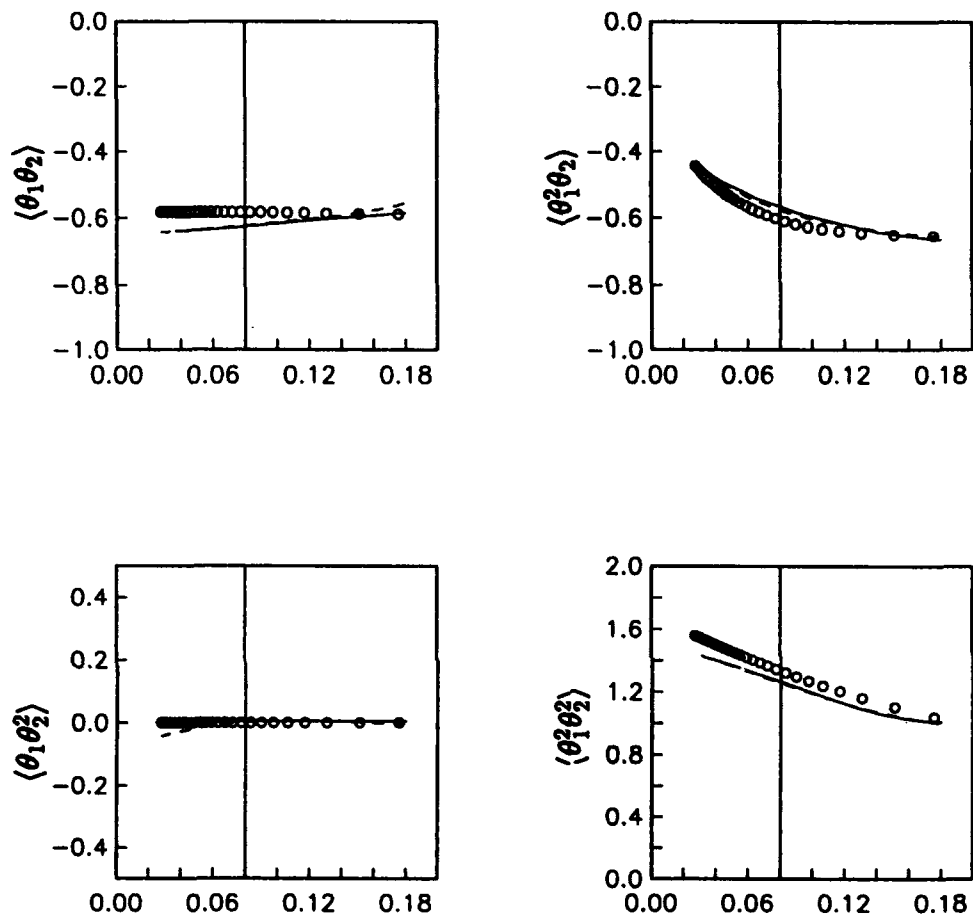
Figure 22: Comparison of mapping closure model and β-pdf model using DRS data for Case C3. Data (soild line), mapping-closure model (- - -) and β-pdf model (circle).
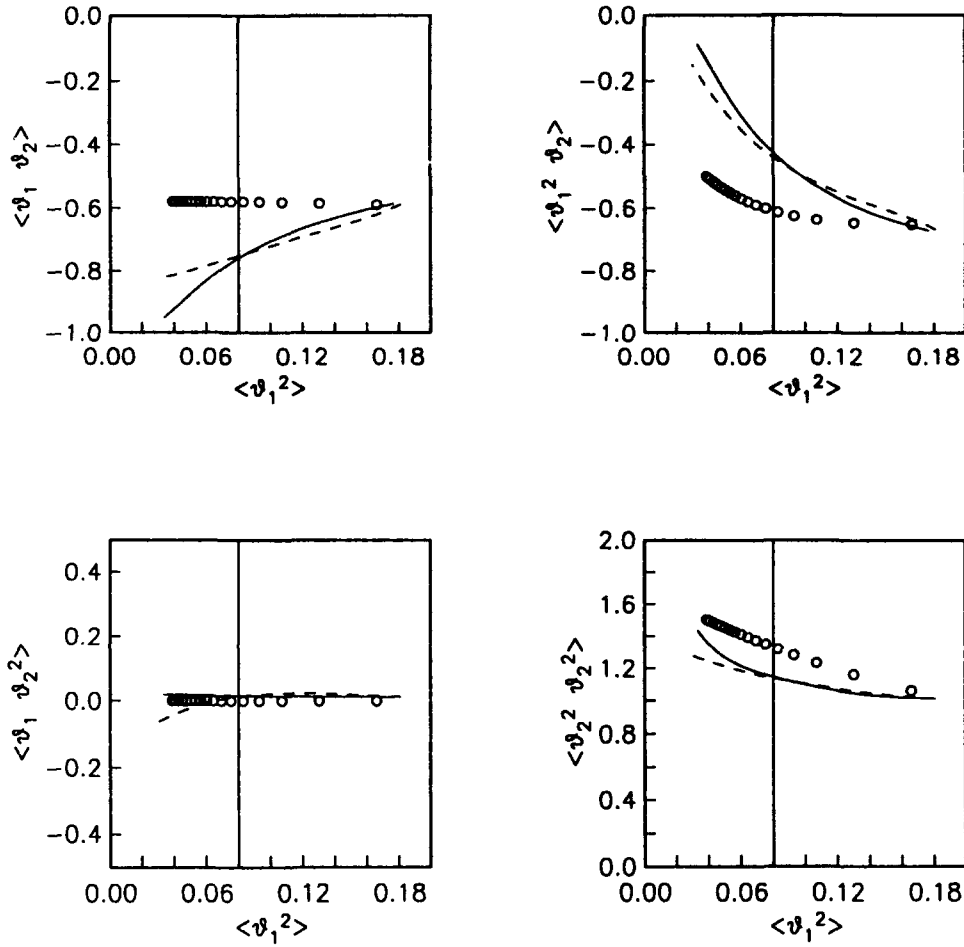
Figure 23: Comparison of mapping closure model and β-pdf model using DRS data for Case C4. Data (soild line), mapping-closure model (- - -) and β-pdf model (circle).

REPORT DOCUMENTATION PAGE

Public reporting burden for this collection of information is estimated to average 1 hour per response, including the time for reviewing instructions, searching existing data sources, gathering and maintaining the data needed, and completing and reviewing the collection of information. Send comments regarding this burden estimate or any other aspect of this collection of information, including suggestions for reducing this burden, to Washington Headquarters Services, Directorate for Information Operations and Reports, 1215 Jefferson Davis Highway, Suite 1204, Arlington, VA 22202-4302, and to the Office of Management and Budget, Paperwork Reduction Project (0704-0188), Washington, DC 20503

1. AGENCY USE ONLY(Leave blank)	2. REPORT DATE October 1993	3. REPORT TYPE AND DATES COVERED Contractor Report

4. TITLE AND SUBTITLE
SIMULATIONS OF DIFFUSION-REACTION
EQUATIONS WITH IMPLICATIONS TO TURBULENT
COMBUSTION MODELING

5. FUNDING NUMBERS

C NAS1-19480
WU 505-90-52-01

6. AUTHOR(S)
Sharath S. Girimaji

7. PERFORMING ORGANIZATION NAME(S) AND ADDRESS(ES)
nstitute for Computer Applications in Science
and Engineering
Mail Stop 132C, NASA Langley Research Center
Hampton, VA 23681-0001

8. PERFORMING ORGANIZATION REPORT NUMBER

ICASE Report No. 93-72

9. SPONSORING/MONITORING AGENCY NAME(S) AND ADDRESS(ES)
National Aeronautics and Space Administration
Langley Research Center
Hampton, VA 23681-0001

10. SPONSORING/MONITORING AGENCY REPORT NUMBER

NASA CR-191536
ICASE Report No. 93-69

11. SUPPLEMENTARY NOTES
Langley Technical Monitor: Michael F. Card
Final Report
To be submitted to Theoretical and Computational Fluid Dynamics

12a. DISTRIBUTION/AVAILABILITY STATEMENT

Unclassified–Unlimited

Subject Category 34

12b. DISTRIBUTION CODE

13. ABSTRACT (Maximum 200 words)
An enhanced diffusion-reaction reaction system (DRS) is proposed as a statistical model for the evolution of multiple scalars undergoing mixing and reaction in an isotropic turbulence field. The DRS model is close enough to the scalar equations in a reacting flow that other statistical models of turbulent mixing that decouple the velocity field from scalar mixing and reaction (e.g. mapping closure model, assumed-pdf models) cannot distinguish the model equations from the original equations. Numerical simulations of DRS are performed for three scalars evolving from non-premixed initial conditions. A simple one-step reversible reaction is considered. The data from the simulations are used (i) to study the effect of chemical conversion on the evolution of scalar statistics, and (ii) to evaluate other models (mapping-closure model, assumed multivariate β-pdf model).

14. SUBJECT TERMS
turbulent combustion modeling; scalar mixing; mixing/reaction

15. NUMBER OF PAGES
44

16. PRICE CODE
A03

17. SECURITY CLASSIFICATION OF REPORT Unclassified	18. SECURITY CLASSIFICATION OF THIS PAGE Unclassified	19. SECURITY CLASSIFICATION OF ABSTRACT	20. LIMITATION OF ABSTRACT

NSN 7540-01-280-5500